ARTICLE IN PRESS

Quaternary International xxx (xxxx) xxx

Contents lists available at ScienceDirect

Quaternary International

journal homepage: www.elsevier.com/locate/quaint

The *Mammuthus-Coelodonta* Faunal Complex at its southeastern limit: A biogeochemical paleoecology investigation in Northeast Asia

Jiao Ma [a,b], Yuan Wang [a,b], Gennady F. Baryshnikov [c], Dorothée G. Drucker [d], Krista McGrath [e,f], Hanwen Zhang [g,h], Hervé Bocherens [d,i,**], Yaowu Hu [j,k,*]

[a] *Key Laboratory of Vertebrate Evolution and Human Origins of Chinese Academy of Sciences, Institute of Vertebrate Paleontology and Paleoanthropology, Chinese Academy of Sciences, Beijing, 100044, China*
[b] *CAS Center for Excellence in Life and Paleoenvironment, Beijing, 100044, China*
[c] *Zoological Institute, Russian Academy of Sciences, Universitetskaya nab. 1, Saint Petersburg, 199034, Russia*
[d] *Senckenberg Centre for Human Evolution and Palaeoenvironment (HEP), Universität Tübingen, Tübingen, 72074, Germany*
[e] *BioArCh, Department of Archaeology, University of York, Heslington, Y010 5DD, UK*
[f] *Departament de Prehisòtria and Institut de Ciència i Tecnologia Ambientals, Universitat Autònoma de Barcelona, Bellaterra, 08193, Spain*
[g] *School of Earth Sciences, University of Bristol, Wills Memorial Building, Bristol, BS8 1RJ, UK*
[h] *Department of Earth Sciences, Natural History Museum, Cromwell Road, London, SW7 5BD, UK*
[i] *Fachbereich Geowissenschaften, Forschungsbereich Paläobiologie, Universität Tübingen, Tübingen, 72074, Germany*
[j] *Institute of Archaeological Sciences, Fudan University, Shanghai, 200433, China*
[k] *Department of Cultural Relics and Museology, Fudan University, Shanghai, 200433, China*

ARTICLE INFO

Keywords:
Northeast Asia
Paleoecology
Mammuthus-Coelodonta Faunal Complex
Bubalus
Carbon and nitrogen stable isotopes
Radiocarbon dates
ZooMS

ABSTRACT

During the past several decades, the paleoecology of the *Mammuthus-Coelodonta* Faunal Complex in the Palearctic has been thoroughly explored, especially using stable isotope analysis. Numerous studies have documented high ecological plasticity and regional heterogeneities for this fauna. However, very limited attention has focused on Northeast Asia, at the southeastern edge of the distribution of the mammoth steppe biome. In the present study, we undertook radiocarbon dating, zooarchaeology by mass spectrometry (ZooMS), and stable isotope analysis on the fossil faunas from Yanjiagang Paleolithic site, Northeast (NE) China, and from the Geographical Society Cave in the nearby Russian Far East, to explore the paleoecology of this fauna in this middle-latitude region. Isotopic ($\delta^{13}C$, $\delta^{15}N$) data from these two sites suggested that the woolly mammoth (*Mammuthus primigenius*) was a grazer feeding on grasses/sedges, while the woolly rhinoceros (*Coelodonta antiquitatis*) and steppe bison (*Bison priscus*) utilized a wider range of food resources. All megaherbivores exhibited some ecological plasticity. Meanwhile, the mammal remains from Geographical Society Cave prevalently exhibited lower $\delta^{15}N$ values than those from China, indicating variable environments and vegetation in Northeast Asia during MIS 3. Interestingly, through reevaluating the diachronic mammal distribution and ecology based on direct radiocarbon dating and ZooMS, we report the credible presence of *Bubalus*, typically interpreted as a mild climate faunal element in the Pleistocene, within the *Mammuthus-Coelodonta* Faunal Complex in Yanjiagang. This emphasizes the unique scenario of this biome in Northeast Asia, where the fauna exhibited sensitivity to synergic effects of climatic oscillations and local geographic traits. After comparing isotopic data of mammoth from different subregions of Asia, we found that NE China displayed both highest $\delta^{13}C$ and $\delta^{15}N$ values, possibly related to the higher temperature compared to the Arctic regions. This study reveals the characteristics and complexity at the southeastern limit of the range of the mammoth steppe biome and urges more systematic studies within and outside this region.

* Corresponding author. Institute of Archaeological Sciences, Fudan University, Shanghai, 200433, China.
** Corresponding author. Universität Tübingen, Hölderlinstr.12, 72074, Tübingen, Germany.
E-mail addresses: herve.bocherens@uni-tuebingen.de (H. Bocherens), ywhu@ucas.ac.cn (Y. Hu).

https://doi.org/10.1016/j.quaint.2020.12.024
Received 29 June 2020; Received in revised form 13 December 2020; Accepted 14 December 2020
Available online 23 December 2020

1. Introduction

The *Mammuthus-Coelodonta* Faunal Complex dominated middle- and high latitude regions of Eurasia during the Late Pleistocene (Kahlke, 2014). This fauna typically contained the emblematic Ice Age megaherbivores *Mammuthus primigenius* (woolly mammoth) and *Coelodonta antiquitatis* (woolly rhinoceros), as well as other cold-adapted mammals (Kahlke, 1999). The use of the terminology *Mammuthus-Coelodonta* Faunal Complex is restricted to Eurasia because of the absence of *Coelodonta* in North America (Stuart and Lister, 2012), where the symbolic woolly mammoth was also present (Lister and Sher, 2001, 2015). With this abundance of the woolly mammoth, the vast areas extending 40 degrees of latitude in the Northern Hemisphere was named as "mammoth steppe" (Guthrie, 2001, 2013; Zimov et al., 2012a, b). As the most thriving and productive biome on Earth, this widespread northern ecosystem disappeared, while most of its large body mass species strongly declining or vanishing at the end of the Pleistocene (Zimov et al., 2012a, b). According to the recent review by Stuart (2015), 37% of mammal species above 45 kg disappeared in northern Eurasia and 69% in Yukon-Alaska. To understand this megafauna extinction event, it is necessary to investigate exhaustively how this ecosystem functioned and fluctuated along with climatic oscillations and geographical differences (Owen-Smith, 1987; Barnosky, 2004; MacDonald et al., 2012; Mann et al., 2013; Stuart, 2015).

As the two most significant aspects of mammalian ecology, habitat and feeding behavior elucidate deep interactions between paleoecology, paleoenvironment, and evolutionary history in the context of understanding extinction risks and mechanisms. During the past several decades, the paleoecology of this fauna has been intensively explored through various methods, such as dental microwear and stable isotope analysis, pollen and spore analysis of feces, as well as stomach content and taphonomic analysis (Guthrie, 1982; Vereshchagin and Baryshnikov, 1982, 1991; Bocherens, 2003; Rivals et al., 2010, 2019; Ukraintseva, 2013, etc). Evidently, the woolly mammoth has been a keystone fossil species that attracted much scientific interest (van Geel et al., 2008; Kirillova et al., 2016; Fisher, 2018; Rivals et al., 2019). However, comparable investigations on the woolly rhinoceros and other sympatric herbivores across a vast region remain limited (Tiunov and Kirillova, 2010; Boeskorov et al., 2011a).

Frozen remains of mammoths and woolly rhinoceros from Siberia have revealed their grass-dominated diet (Boeskorov et al., 2011a; Kosintsev et al., 2012). However, dental mesowear and microwear analysis has indicated that they were not only strict grazers, but instead exploited various food resources in a flexible way (Rivals and Lister, 2016; Saarinen et al., 2016; Saarinen and Lister, 2016; Rivals and Álvarez-Lao, 2018). Stable isotope analysis has provided key information to this topic since it allows the paleoecological reconstruction at the scale of individual animals (Bocherens, 2002). Carbon and nitrogen stable isotope analysis on collagen of this fauna revealed that mammoths had significantly higher $\delta^{15}N$ values and relatively low $\delta^{13}C$ values compared to other herbivores, based on numerous investigations initiated since the 1990s and covering most regions where the mammoth steppe biome was once present (e.g. Bocherens et al., 1991; 1994; 1996; 1997; 2015b; Iacumin et al., 2000; 2010; Szpak et al., 2010; Metcalfe et al., 2013; Arppe et al., 2011; 2019; Schwartz-Narbonne et al., 2019; Widga et al., 2020). It has been speculated that this isotopic pattern resulted from the specialized dietary resources exploited by woolly mammoth (Schwartz-Narbonne et al., 2015; Naito et al., 2016). However, in some cases, mammoth $\delta^{15}N$ values were equal or even lower than those of horses, which probably corresponded to the decline of mammoth populations in sway with habitat loss at the southern limits of their geographic distribution ca. 18–17 kyrs ago (Drucker et al., 2014, 2018). Summary of the published $\delta^{13}C$ and $\delta^{15}N$ data on the whole biome suggested that the mammoth steppe ecosystem could have had a very high level of functional redundancy (Schwartz-Narbonne et al., 2019), and that ecological flexibility of different species was commonplace (Pushkina et al., 2014; Rivals and Álvarez-Lao, 2018). Therefore, regional faunal ecology should be investigated further, along with the local vegetation and climate history to better understand the evolution of different species in this ecosystem and of the animal community as a whole.

Of special interest are the areas at the southeastern marginal distribution of the *Mammuthus-Coelodonta* Faunal Complex, in middle-latitude Northeast Asia. However, ecological inferences concerning mammoths and other associated mammals have received very scant attention in the recent decades, especially in Northeast (NE) China (Zhang, 2009), even in light of our previous isotopic study on the Late Pleistocene mammoth steppe fossil collections from the Daqing Museum in Heilongjiang Province (Ma et al., 2017). Moreover, the lack of absolute dating of the *Mammuthus-Coelodonta* Faunal Complex from NE China also hampers our understanding of the temporal ecological shifts related to this fauna. For example, new AMS radiocarbon dates of one *Mammuthus* and one *Bison* from Inner Mongolia were almost 10,000 years older than stated in previous work (Zhang et al., 2019). These new studies underline the need to reevaluate the spatio-temporal distribution of the *Mammuthus-Coelodonta* Faunal Complex in China. Meanwhile, this fauna has previously been intensively investigated in Siberia, but prior studies mostly focused on the high-latitude regions (Arppe et al., 2019; Kuitems et al., 2019). In NE China, the *Mammuthus-Coelodonta* Faunal Complex is characterized by an unusual abundance of woolly rhinoceros and/or bovines in many sites, as well as the sparse presence of species usually considered mild climate elements (Tang et al., 2003; Chen et al., 2016; Zhang et al., 2016, 2019). In southern Far East Russia, paleontological studies also found a high species diversity (Baryshnikov, 2014; 2015a; b, 2016). This emphasizes the need to explore all aspects of the *Mammuthus-Coelodonta* Faunal Complex in this special marginal region of the mammoth steppe.

In the present study, we performed the stable isotope analysis on the faunal remains from Paleolithic site of Yanjiagang in NE China, as well as the Geographical Society Cave site in the southern Russian Far East to explore the paleobiology of the *Mammuthus-Coelodonta* Faunal Complex in this region. To better investigate this fauna in Northeast Asia, radiocarbon dating and ZooMS analysis were applied on the same materials and combined with the isotopic investigation. Finally, the interactions between mammalian ecology, climatic oscillations, and paleoenvironment will be discussed thoroughly within and outside the context of the study region.

2. Materials and methods

2.1. Materials

2.1.1. Yanjiagang

Although China holds plenty of fossil localities pertained to the *Mammuthus-Coelodonta* Faunal Complex, many of them lack clear contexts and accurate radiocarbon dates (Liu and Li, 1984; Tong and Patou-Mathis, 2003; Zhang, 2009). This regrettably compromised situation pales in comparison to the exhaustive studies on this fauna globally, and thus impeded the research on megafauna extinction in China at the end of the Quaternary (Turvey et al., 2013).

Located in Harbin Municipality, Heilongjiang Province, the Yanjiagang site (45°36′E, 126°18′N, see in Fig. 1) was systematically excavated in the early 1980s, leading to the discovery of large amounts of animal bones and human-made lithic artefacts. The most fascinating discoveries in this site are two semi-circular structures formed from hundreds of animal bones (mainly bison, woolly rhinoceros, and horse remains, including skeletal elements from subadult individuals), named HY84TA3 and HY84T4 (Heilongjiang Cultural Relics Management Committee, 1987). Debates remain around the formation of these two semicircular heaps, with many scholars arguing they were constructed intentionally by ancient hunter-gatherers to butcher their prey (and therefore, Yanjiagang should also be considered as an ancient campsite)

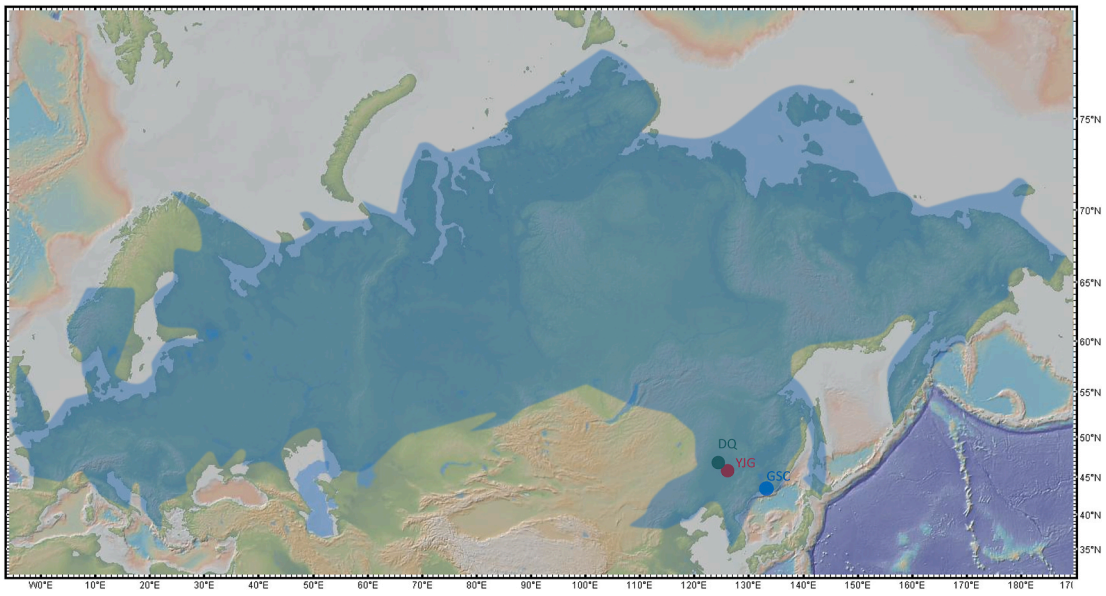

Fig. 1. Map of the three sites in this study. ("DQ" indicates "Daqing Museum", "YJG" indicates "Yanjiagang", "GSC" indicates "Geographical Society Cave"; The blue shaded area represents the distribution of the *Mammuthus-Coelodonta* Faunal Complex. Figure was modified from GeoMapApp www.geomapapp.org). (For interpretation of the references to colour in this figure legend, the reader is referred to the Web version of this article.)

(Heilongjiang Cultural Relics Management Committee, 1987). Other researchers argued that this structures resulted from a combination of freeze-thaw action and water transportation (Huang, 2008; Yu et al., 2010; Wei et al., 2012). The fauna remains at Yanjiagang are dominated by *Bison priscus* (NISP: 604) and *C. antiquitatis* (NISP: 129). The herbivore remains from Yanjiagang are mostly broken, possibly damaged by carnivores or/and early humans. The age of Yanjiagang was previously dated to 26,957 ± 626 cal BP determined by radiocarbon dating of a mammal bone sample (Heilongjiang Cultural Relics Management Committee, 1987), with following five radiocarbon dates ranging from >41,300 yr BP to 26,560 ± 670 yr BP without complete publication (Ives et al., 1994). In this study, we selected 42 herbivore samples without clear ontogenetic identification of subadults from Yanjiagang, including *M. primigenius* (n = 10), *C. antiquitatis* (n = 17, from 16 individuals), the steppe bison *B. priscus* (n = 12), and the caballine horse *Equus* cf. *przewalskii* (n = 3) (see Table 1). These taxonomic determinations were originally based on morphological characteristics, but several of them were corrected following ZooMS investigations during the course of this work (see Table 1).

2.1.2. Geographical Society Cave

We selected Geographical Society Cave (42°52′N, 133°00′E, also see in Fig. 1) located in the southern part of Primorsky Territory as a representative site of the Russian Far East (Baryshnikov, 2014; 2015a; b, 2016), situated at a lower latitude than Yanjiagang. Geographical Society Cave was discovered by the Partizanskaya River, containing stone and bone tools, and also large amounts of animal bones. 36 mammal species were excavated from Geographical Society Cave, including the emblematic *M. primigenius, C. antiquitatis*, and *B. priscus,* along with a very abundant cervid assemblage as well as carnivores (Ovodov, 1977; Baryshnikov, 2014, 2015a, b, 2016). Previous radiocarbon dates had assigned the time of formation of the bone-bearing layer as MIS 3 (40,000 to 30,000 uncal BP) (Kuzmin et al., 2001; Baryshnikov, 2014). Ten herbivores specimens were selected from Geographical Society Cave for preliminary analysis, including *M. primigenius* (n = 1), *C. antiquitatis* (n = 2), *B. priscus* (n = 3), *Equus* sp. (n = 1), moose (*Alces alces*, n = 1), and the Northeast Asian wapiti (*Cervus xanthopygus*, n = 2) (See in Table 1). All the samples were bones except for a mammoth sample from a DP3/4 dentine.

2.2. Collagen extraction

Collagen was extracted following a well-established protocol based on Bocherens et al. (1991, 1997) at the University of Tübingen. A small fragment (~500 mg) was carefully sampled with a rotary tool bearing a circular diamond-coated blade. The samples were ultrasonicated in acetone in order to remove possible synthetic glue, then rinsed with distilled water then dried and powdered to a particle size of less than 0.7 mm. To screen a large number of specimens for the quality of collagen preservation, a preliminary determination of the total nitrogen (N) content was performed, as suggested by Iacumin et al. (1996). 5–7 mg powder of each sample was measured on a CHN elemental analyzer Carlo Erba NA 1500. The samples with qualified N contents (higher than 0.4%) were chosen to extract collagen as described in the following steps. Namely, 200–500 mg of bone powder (the weight was determined based on the nitrogen content) was decalcified in 1 M HCl for 20 min at room temperature and filtered through a 5 mm filter. The insoluble residue was then soaked in 0.125 M NaOH for 20 h at room temperature. Subsequently, the rinsed residue was heated in closed tubes at 100 °C for 17 h in HCl pH2 solution, in order to gelatinize the collagen. After filtration through a 5 mm filter, the filtrate containing gelatinized collagen was freeze-dried.

2.3. Stable isotopic analysis

Collagen samples from Yanjiagang were measured in the Archaeological Stable Isotope Laboratory, Department of Archaeology and Anthropology, University of Chinese Academy of Sciences. Approximately 0.6–1 mg of extracted collagen was weighed out for each sample, and the elemental contents and stable isotope ratios of carbon and nitrogen of each collagen specimens were measured on an IsoPrime-100 isotope ratio mass spectrometer (IRMS) coupled with Elementar Vario. International standards, including Acetanilide, IAEA-600, IAEA-N-2, IAEA–CH–6, USGS 40, and USGS 41 were used for elemental and isotopic calibration (two-point normalization), as well as one collagen lab standard (δ^{13}C value: −14.7 ± 0.2‰, δ^{15}N value: +7.0 ± 0.2‰). The long-term measurement precisions of the δ^{13}C and δ^{15}N values are less than ±0.2‰.

The samples from Geographical Society Cave were measured at the Department of Geosciences of the Universität Tübingen, on an NC2500

Table 1
Sample information with morphological and ZooMS identification, and sable isotope analysis of the *Mammuthus-Coelodonta* Faunal Complex in Yanjiagang (YJG) and Geographical Society Cave (GSC). N/A denotes samples not analyzed with ZooMS.

Lab No.	Original No.	Identification		Anatomical determination	Collagen yields (%)	%C	%N	Atomic C/N	$\delta^{13}C$	$\delta^{15}N$
		Morphological	ZooMS							
YJG-02	HY84#1-8	*Mammuthus primigenius*	*Mammuthus primigenius*	broken humerus	10.2	42.2	15.5	3.2	−21.5	13.1
YJG-10	HY84T5-18	*Mammuthus primigenius*	*Mammuthus primigenius*	broken metacarpal	10.3	38.8	14.4	3.1	−21.2	12.1
YJG-15	HY85T2-0057	*Coelodonta antiquitatis*	*Mammuthus primigenius*	unknown long bone	12.3	39.2	14.5	3.1	−20.7	9.2
YJG-03	HY84T4-01	*Mammuthus primigenius*	*Coelodonta antiquitatis*	possible broken humerus	12.7	41.5	15.5	3.1	−20.7	7.5
YJG-01	HY85T1-0023	*Mammuthus primigenius*	*Coelodonta antiquitatis*	possibly broken radius	12.4	41	14.9	3.2	−20.8	7.7
YJG-05	HY84T4-17(R)	*Mammuthus primigenius*	*Coelodonta antiquitatis*	right broken ulna	13.1	40.7	14.9	3.2	−20.7	7.6
YJG-06	HY85T1-0011	*Mammuthus primigenius*	*Coelodonta antiquitatis*	broken radius	13.1	41.7	15.3	3.2	−20.9	7.6
YJG-07	HY84T4-19	*Mammuthus primigenius*	*Coelodonta antiquitatis*	left broken ulna	9.1	39.8	14.5	3.2	−21	8.7
YJG-08	HY85T1-0044	*Mammuthus primigenius*	*Coelodonta antiquitatis*	broken pelvis	12.4	40.4	14.7	3.2	−20.8	8.3
YJG-09	HY84T4-13	*Mammuthus primigenius*	*Coelodonta antiquitatis*	unknown	14.4	42.4	15.4	3.2	−20.9	10.9
YJG-13	HY82C 124 (R)	*Coelodonta antiquitatis*	*Coelodonta antiquitatis*	possible broken tibia	11.3	40	15.1	3.1	−21.2	6.4
YJG-18	HY84T4-19(L)	*Coelodonta antiquitatis*	*Coelodonta antiquitatis*	possibly humerus	16.4	39.8	14.5	3.2	−21	8.5
YJG-21	T4-03	*Coelodonta antiquitatis*	*Coelodonta antiquitatis*	unknown long bone	12.1	40	14.8	3.2	−20.3	8.4
YJG-23a	HY84#1-69	*Coelodonta antiquitatis*	*Coelodonta antiquitatis*	broken mandible	12.1	40.6	15	3.2	−19.8	11.9
YJG-23b	HY84#1-69	*Coelodonta antiquitatis*	*Coelodonta antiquitatis*	dp4	10.0	38.6	13.9	3.2	−20.1	11.7
YJG-11	HY84T4 57-I (L)	*Coelodonta antiquitatis*	N/A	left broken ulna	15.9	40.9	14.9	3.2	−20.7	8.9
YJG-12	HY84T4 5(R)	*Coelodonta antiquitatis*	N/A	right broken humerus	12.9	41.1	15.2	3.2	−20.7	8.6
YJG-14	HY82C 102(R)	*Coelodonta antiquitatis*	N/A	broken radius	10.6	40.5	14.7	3.2	−20.8	10.2
YJG-16	HY84 #1–11 (R)	*Coelodonta antiquitatis*	N/A	right broken humerus	12.1	41.1	15.1	3.2	−20.3	10.1
YJG-20	HY84T4-03	*Coelodonta antiquitatis*	N/A	broken humerus	12.7	39	14.7	3.1	−21	8.4
YJG-22	HY84T4-16(R)	*Coelodonta antiquitatis*	N/A	right broken radius	16.5	40.2	14.8	3.2	−20.6	9.2
YJG-24	HY84#1–7(R)	*Coelodonta antiquitatis*	N/A	broken tibia	15.7	37.4	13.8	3.2	−20.7	10
YJG-25	HY84T4-8	*Coelodonta antiquitatis*	N/A	broken mandible	15.0	39.8	14.7	3.1	−20.9	10.3
YJG-27	82HYMT1:73	*Bison priscus*	*Bison priscus*	broken metatarsal	16.3	40.5	14.8	3.2	−20.4	10.1
YJG-32	83HYTB3:24	*Bison priscus*	*Bison priscus*	broken humerus	14.0	40.5	14.9	3.2	−20.7	9.9
YJG-33	HY84T2-54	*Bison priscus*	*Bison priscus*	broken metatarsal	12.8	31	12.2	3	−21.3	9.6
YJG-34	HY84#1-29	*Bison priscus*	*Bison priscus*	unknown long bone	13.7	40.5	14.8	3.2	−19.3	8.4
YJG-36	HY82C 202	*Bison priscus*	*Bison priscus*	broken tibia	14.9	40	14.7	3.2	−19.7	5.5
YJG-40	HY85-0128	*Equus* sp. (cf. *E. przewalskii*)	*Bison priscus*	broken ulna	10.4	40.3	14.8	3.2	−20	9.3
YJG-26	83HYT, B,3:80	*Bison priscus*	N/A	broken tibia	12.3	40.2	15	3.1	−19.8	7.3
YJG-28	HY82C:205	*Bison priscus*	N/A	broken ulna	15.4	41	15.2	3.2	−19.2	9.2
YJG-29	HY84T4 40-9	*Bison priscus*	N/A	broken radius	3.9	39.2	14.3	3.2	−20.1	9.5
YJG-30	HY85T1-0004	*Bison priscus*	N/A	broken ulna	13.9	41.4	15.3	3.1	−19.9	10.1
YJG-35	83HYTA4:59	*Bison priscus*	N/A	broken radius	11.6	39	14.5	3.1	−19.4	8.4
YJG-37	HY82C,198	*Bison priscus*	N/A	broken metatarsal	10.5	40.7	15	3.2	−19.8	8.9
YJG-19	83HYTA4:51	*Equus* sp. (cf. *E. przewalskii*)	*Equus* sp. (cf. *Equus przewalskii*)	broken pelvis	13.1	37.9	13.7	3.2	−21.5	9.3
YJG-38	HY84#1-9	*Bison priscus*	*Equus* sp. (cf. *Equus przewalskii*)	unknown long bone	13.9	39.5	14.5	3.2	−21.3	8.4
YJG-39	Unknown	*Equus* sp. (cf. *E. przewalskii*))	*Equus* sp. (cf. *Equus przewalskii*)	broken humerus	10.7	39.9	14.7	3.2	−21.3	5.6
YJG-41	81HYTA4:65	*Equus* sp. (cf. *E. przewalskii*)	*Equus* sp. (cf. *Equus przewalskii*)	unknown vertebrate	13.1	44.7	16.4	3.2	−21.4	7.9
YJG-04	HY85T1-0045	*Mammuthus primigenius*	*Bubalus* sp. (cf. *Bubalus wansjocki*)	broken cervical vertebra	17.2	40.6	14.9	3.2	−19.4	9.8
GSC-21	Coll. ZIN RAS	*Mammuthus primigenius*	N/A	dental plate of DP3/4	7.8	40	14.1	3.3	−20.9	9.9
GSC-19	Coll. ZIN RAS	*Coelodonta antiquitatis*	N/A	ulna	10.6	28.3	9.9	3.4	−20.7	4.7

(*continued on next page*)

Table 1 (*continued*)

Lab No.	Original No.	Identification		Anatomical determination	Collagen yields (%)	%C	%N	Atomic C/N	$\delta^{13}C$	$\delta^{15}N$
		Morphological	ZooMS							
GSC-20	Coll. ZIN RAS	*Coelodonta antiquitatis*	N/A	humerus	12.9	41.2	14.8	3.3	−20.1	4.5
GSC-17	Coll. ZIN RAS	*Equus* sp.	N/A	metacarpal	10.8	43.5	15.6	3.3	−21.5	5.4
GSC-18	Coll. ZIN RAS	*Bison priscus*	N/A	humerus	7.9	45	16.2	3.2	−20.1	5.4
GSC-15	Coll. ZIN RAS	*Bison priscus*	N/A	metatarsal	9.7	43.7	15.1	3.4	−20.1	5.2
GSC-16	Coll. ZIN RAS	*Bison priscus*	N/A	metatarsal	7.0	41.2	14.5	3.3	−20.1	4.9
GSC-13	Coll. ZIN RAS	*Alces alces*	N/A	metapodial	9.3	41.1	14.3	3.3	−20.3	2.9
GSC-11	Coll. ZIN RAS	*Cervus xanthopygus*	N/A	metapodial	7.7	41.5	14.5	3.4	−20.3	4.9
GSC-12	Coll. ZIN RAS	*Cervus xanthopygus*	N/A	metapodial	8.2	41.8	14.7	3.3	−20.3	5.3

elemental analyzer coupled to a Thermo Quest Delta þ XL IRMS. Measured $\delta^{13}C$ and $\delta^{15}N$ data were calibrated to the recognized values of international reference materials and in-house reference materials, using a two-point calibration scheme. An in-house acetanilide material ($\delta^{13}C = -30.0‰$; $\delta^{15}N = -1.0‰$), USGS-24 ($\delta^{13}C = -16.0‰$), and IAEA-N-2 ($\delta^{15}N = +20.3‰$) were used. The calibration references indicate an internal precision (SD, 1s) of ±0.1‰ for $\delta^{13}C$ and ±0.2‰ for $\delta^{15}N$ values. The analyzed (n = 10) quality control materials indicate an external reproducibility (SD, 1s) of ±0.1‰ for $\delta^{13}C$ and ±0.2‰ for $\delta^{15}N$ values.

Additionally, collagen extraction was performed on two in-house bone powder reference samples (camel and elk) to check for consistency of extraction, chemical composition, and isotopic composition among measurement series for both sites. All isotope data are given in the δ notation as permil (‰), relative to the VPDB standard for carbon and AIR for nitrogen.

2.4. ZooMS analysis

At the Yanjiagang site, most bone specimens are fragmented. Considering this, we applied ZooMS analysis to redress any possible misidentification of these broken bones. Collagen remaining from isotopic analysis was subsampled (2–3 mg) from 25 selected samples and sent to the BioArCh facilities in the Department of Archaeology at the University of York, UK. ZooMS was performed following a modified method from that in Buckley et al., (2009), with 0.3–0.7 mg of collagen resuspended in 50 μl of ammonium bicarbonate buffer (50 mM, pH 8) and digested with 0.4 μg of trypsin overnight at 37 °C. Samples were acidified to stop digestion with 1 μl of 5% TFA, and the peptides were eluted using C18 Zip Tips (EMD Millipore). 1 μl of sample was mixed with 1 μl of matrix solution (α-cyano-hydroxycinnamic acid) and spotted in triplicated along with calibration standards, then analyzed on a Bruker Ultraflex III MALDI-TOF-MS. Triplicate spectra were averaged and analyzed using mMass software (Strohalm et al., 2008), with taxonomic identifications made through comparison with known collagen peptide markers (Buckley et al., 2009; Kirby et al., 2013; Welker et al., 2016).

2.5. AMS ^{14}C dating

Based on the isotopic pattern, we selected seven samples with accurate ZooMS identification and representative isotopic results for radiocarbon dating. Remaining collagen samples from previous analyses were subsampled, with 5–10 mg sent to the Laboratory of Ion Beam Physics in Zurich, Switzerland. Of particular note here is that all the collagen sent for radiocarbon dates yielded C content above 30%, ranging from 38.8% to 42.4%, as recommended by van Klinken in 1999.

3. Results

3.1. Collagen preservation

Only two samples contained less than 0.4% nitrogen among all the 52 bones sampled in Yanjiagang and Geographical Society Cave, with well-preserved collagen successfully extracted from the other 50 samples. The atomic C/N ratio of the collagen of the samples ranged from 3.0 to 3.4 (C% = 28.3–45.0% and N% = 9.9–16.4%), the collagen yield rates were averaged by 12.1 ± 2.8%, as shown in Table 1. All parameters indicated a very good quality of collagen (DeNiro, 1985; van Klinken, 1999; van der Plicht and Palstra, 2016).

3.2. ZooMS identification at Yanjiagang

All 25 collagen samples were successfully identified using ZooMS, with the results indicating that 12 samples had previously been misidentified based on morphology (see Table 1 and Fig. 2a). We also supplied the peptide markers in Supplementary Table 1 and the example spectra in Supplementary Figs. 1 and 2. Even though ZooMS cannot distinguish between closely related taxa as such, contextual information along with evidence from the overall faunal assemblage has been applied to the ZooMS species identifications listed in Table 1 (see Supplementary Table 1 for original ZooMS identifications). Therefore, for specimens identified as rhino the most likely species is woolly rhinoceros (*C. antiquitatis*), for those identified as elephant the most likely species is woolly mammoth (*M. primigenius*), for those identified as cattle (*Bos* sp.) the most likely species is steppe bison (*B. priscus*), and for those identified as horse the most likely species is Przewalski's horse (*E. przewalskii*).

In addition, ZooMS identified one previously misidentified woolly mammoth specimen as actually belonging to *Bubalus* sp. While the markers used to make this identification refer specifically to *Bubalus bubalis* (as it is the only *Bubalus* sp. with ZooMS markers currently available), contextually, this sample is likely to be *Bubalus wansjocki* as inferred from the fauna composition of Yanjiagang, where only one fragment of buffalo horn core was identified (Heilongjiang Cultural Relics Management Committee, 1987). The buffalo bone identified in this study represents a further case of coexistence of buffalo with the *Mammuthus-Coelodonta* Faunal Complex. Therefore, as demonstrated in previous studies (Fellows Yates et al., 2017), ZooMS analysis provides a highly recommended procedure for accurately identifying morphologically indeterminate mammal remains.

3.3. Stable isotope results

The results of the stable isotopic analysis are also shown in Table 1 and Fig. 2. In Yanjiagang, the $\delta^{13}C$ values of the fauna ranged from −21.5‰ to −19.2‰, n = 40, while the $\delta^{15}N$ values were distributed from +5.5‰ to +13.1‰ (see Fig. 2a). Three mammoths had $\delta^{13}C$ and $\delta^{15}N$ values averaging −21.1 ± 0.4‰ and +11.5 ± 2.0‰, respectively. Woolly rhinoceros exhibited $\delta^{13}C$ values ranging from −21.2‰ to −19.8‰, averaging −20.7 ± 0.3‰ (n = 20); while their $\delta^{15}N$ values were more widely distributed from +6.4‰ to +11.9‰, with a mean of +9.0 ± 1.5‰ (n = 20). The steppe bison had the highest $\delta^{13}C$ mean values of −20.0 ± 0.6‰ (n = 12) and also quite high $\delta^{15}N$ values (+8.8 ± 1.3‰) compared to the woolly rhinoceros. Similarly, the distribution of $\delta^{13}C$ and $\delta^{15}N$ values of the steppe bison was wide, ranging from

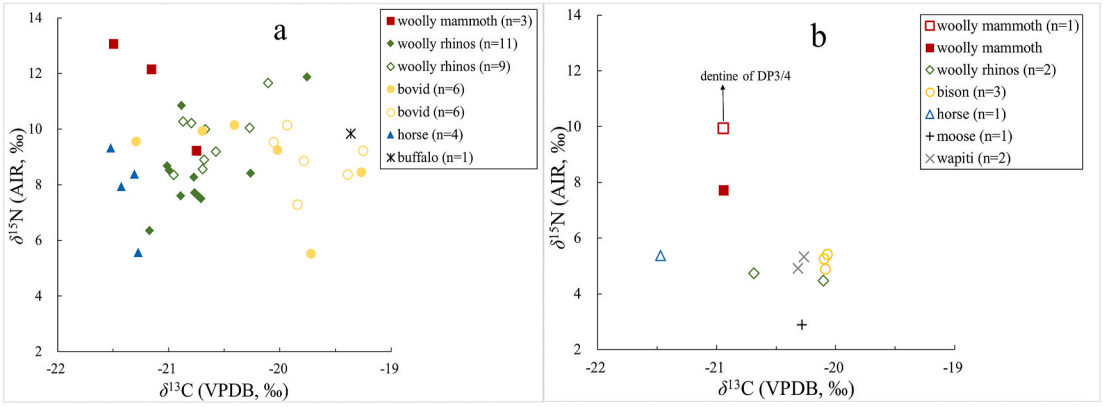

Fig. 2. a, Scatter plot of $\delta^{13}C$ and $\delta^{15}N$ values and ZooMS results of Yanjiagang fauna (solid symbols are identified by ZooMS); b, Scatter plot of $\delta^{13}C$ and $\delta^{15}N$ values of Geographical Society Cave fauna.

−21.3 to −19.2‰ and from +5.5 to +10.1‰, respectively. Horse yielded both the lowest $\delta^{13}C$ and $\delta^{15}N$ values, with −21.4 ± 0.1‰ and +7.8 ± 1.6‰ (n = 4), respectively. The single confirmed buffalo sample yielded both high $\delta^{13}C$ and $\delta^{15}N$ values of −19.4‰ and +9.8‰, respectively. Among the samples distributed at the marginal areas of the isotopic range of a species (see Fig. 2a), many of them were all taxonomically identified by ZooMS, confirming that the scattered isotopic data was not due to misidentifications but rather to true high variation of isotopic values within taxonomic categories.

As seen in Fig. 2b, the ten samples from Geographical Society Cave yielded quite different isotopic signatures compared to Yanjiagang. The only mammoth sample had the highest $\delta^{15}N$ value and a lower $\delta^{13}C$ value, of +9.9‰ and −20.9‰, respectively. The other herbivores clearly showed much lower $\delta^{15}N$ values compared to the mammoth, with horses, woolly rhinoceros, bisons, and wapitis all having $\delta^{15}N$ values around +5‰, with one moose providing the lowest $\delta^{15}N$ value of +2.9‰ (n = 1). Three bison samples had the highest $\delta^{13}C$ values of −20.1‰, while one horse yielded the lowest $\delta^{13}C$ values of −21.5‰. Two woolly rhinoceros samples displayed the intermediate $\delta^{13}C$ values of −20.1‰ and −20.7‰, while three cervids all had the same $\delta^{13}C$ values of −20.3‰.

3.4. AMS ^{14}C dating

All the results of ^{14}C dates are displayed in Table 2. The AMS ^{14}C ages were calibrated into calendar years using the IntCal 20 atmospheric curve on OxCal online (Bronk Ramsey, 2017; Reimer et al., 2020). Seven samples (three mammoths, three woolly rhinoceros, and one buffalo) were dated between 43,447/>41,964 to 38,204 ^{14}C age BP, calibrated as 47,763–44,635 to 42,530–42,145 cal BP (see in Table 2). The seven new dates were all older than the previously published dates (Heilongjiang Cultural Relics Management Committee, 1987; Ives et al., 1994), though all belonged to MIS 3. Two main explanations can be proposed to explain the discrepancy of the dating: first, the site experienced a long-term formation process; second, the previous radiocarbon dates need to be reexamined.

Of particular note here is that these collagen samples were not ultrafiltrated, which was the proper procedure recommended for the ancient bones (Bronk Ramsey et al., 2004). It has been tested that the bones using ultrafiltration techniques normally yielded older radiocarbon dates compared to the samples without ultrafiltration (Higham et al., 2006). Although in some cases no obvious differences were found on the well-preserved collagen. Besides, even slight difference would not influence the discussion in this study relating to MIS 3.

4. Discussion

4.1. Foraging ecology of the Mammuthus-Coelodonta Faunal Complex in Northeast Asia

Hereby, the two sites examined in this study are compared with an additional 28 published data from our previous study of the Daqing Museum collections (Ma et al., 2017, data in Supplementary Table 2; location also shown in Fig. 1), in order to thoroughly discuss the foraging ecology of *Mammuthus-Coelodonta* Faunal Complex in Northeast Asia. Since the Daqing Museum materials analyzed by Ma et al. (2017) were procured from numerous assorted localities mainly in Heilongjiang, NE China, the sample unfortunately lacks provenance information and exact dating, and will be collectively referred to as the Daqing Museum samples hereafter. Although no direct dating was applied to the Daqing Museum samples, at least some of them were highly likely collected from the nearby Qinggang village, where a bone was ^{14}C dated as >43.5 ka (Jiang et al., 2019), so probably

Table 2
AMS ^{14}C dating results of Yanjiagang mammal bones from this and previous studies.

Sample No.	^{14}C No.	Species	^{14}C age BP	±1σ	Calibrated age range (95.4% prob.)
YJG-10	ETH-98609	*Mammuthus primigenius*[a]	38,204	225	42,530–42,145
YJG-02	ETH-98608	*Mammuthus primigenius*[a]	41,103	313	44,590–43,311
YJG-15	ETH-98610	*Mammuthus primigenius*[a]	>41,964		
YJG-04	ETH-102510	*Bubalus* sp.[a]	43,447	833	47,763–44,635
YJG-01	ETH-102509	*Coelodonta antiquitatis*[a]	40,441	579	44,476–42,820
YJG-09	ETH-102511	*Coelodonta antiquitatis*[a]	42,241	721	46,364–43,854
YJG-23A	ETH-102512	*Coelodonta antiquitatis*[a]	42,310	726	46,447–43,949
Not provided		mammal bone	22,370	300	26,957±626[1]
Not fully provided		mammal bones	>41,300 yr BP (AECV-1404) to 26,560 ± 670 yr BP (AECV-1402) (n = 5, full data and sample background information were not provided)[2]		

(Note.
[a] Represents that the taxonomy is confirmed by ZooMS; reference 1: Heilongjiang Cultural Relics Management Committee, 1987, reference 2: Ives et al., 1994).

contemporaneous with our Yanjiagang samples. Considering that mammothswere barely present in China during or after the LGM (Zhang et al., 2019), these samples could be considered as roughly contemporary.

Meanwhile, the Yanjiagang site is located on the Songnen Plain, near the Yunliang River, at an altitude of ~100 meters above sea level (Heilongjiang Cultural Relics Management Committee, 1987). Though lacking clear background information, the samples from Daqing Museum collected from surrounding areas were possibly also originated from similar deposits, because the Quaternary landscape of Heilongjiang Province is dominated by plains and low mountains (Heilongjiang Cultural Relics Management Committee, 1987). The Quaternary mammal fossils from Heilongjiang were mainly found in river terraces, lacustrine deposits, bed facies deposits, and valley basin, all within a few hundred meters in altitude (Heilongjiang Cultural Relics Management Committee, 1987). Based on the different stable isotopic pattern of NE China and Geographical Society Cave, as such the foraging ecology of the faunas will be interpreted in terms of the two subregions.

4.1.1. NE China

The isotopic results from our Daqing Museum samples are similar to Yanjiagang, so when combining these two sites in Fig. 3, the general pattern is in line with Fig. 2a. Even though the data variability could partially result from some degree of temporal heterogeneity of the samples, stable isotopic data from the *Mammuthus-Coelodonta* Faunal Complex in NE China is still consistent with the typical isotopic pattern of the mammoth steppe faunas in other regions (Bocherens, 2003), where woolly mammoths exhibit highest δ^{15}N (+10.7 ± 1.6‰, n = 9) and relatively low δ^{13}C values (−21.4 ± 0.4‰) compared to other herbivores. The sample size of mammoths from Yanjiagang is small comparing to the woolly rhinoceros and bison, due to morphological misidentification prior to the introduction of ZooMS into our study. But the isotopic result are deemed adequate to reflect foraging specialization on grasses/sedges for mammoths, which has been widely documented through multiple paleoecological proxies across the vast mammoth steppe (e.g. van Geel et al., 2008; Kuitems et al., 2012; Schwartz-Narbonne et al., 2015; Rivals et al., 2019). In Yanjiagang, two mammoth samples (YJG-10 and YJG-02) with similar isotopic values (δ^{13}C: 21.2‰, −21.5‰; δ^{15}N: +12.1‰, +13.1‰) were respectively dated to 38,204 ± 225 and 41,103 ± 313 ^{14}C yr BP (42,530–42,145 and 44,590–43,311 cal BP), and thus clearly not contemporary. This also demonstrates that as the iconic mammal of the Ice Age, woolly mammoths occupied a relatively specialized ecological niche across different periods throughout their temporal span.

Overall, woolly rhinoceros are characterized by relatively high δ^{15}N and low δ^{13}C values (δ^{13}C: 20.7 ± 0.3‰, δ^{15}N: +8.9 ± 1.6‰, n = 23), reflecting partially similar feeding preference to woolly mammoths as a grazer consuming grasses/sedges. In Yanjiagang, the distribution of δ^{13}C values for woolly rhinoceros (−21.2 to −19.8‰) are broader than for woolly mammoths (−21.5 to −20.7‰), reflecting a mixed feeding ecology as found in other cases (Tiunov and Kirillova, 2010; Boeskorov et al., 2011b; Rivals and Álvarez-Lao, 2018). In the case of the three dated woolly rhinoceros samples, YJG-09 and YJG-23A had very close radiocarbon ages of 42,241 ± 721 ^{14}C yr BP (46,364–43,854 cal BP) and 42,310 ± 726 ^{14}C yr BP (46,447–43,949 cal BP). However, YJG-23A had both the highest δ^{13}C and δ^{15}N value of −19.8‰ and +11.9‰ among all the 20 woolly rhinoceros specimens analyzed in this study, differing from YJG-09 which had lower δ^{13}C and δ^{15}N values (−20.9‰, +10.9‰). Such disparity could also evidence the more flexible foraging ecology of the woolly rhinoceros, compared to the woolly mammoth. A partial overlap in the isotopic values of the two species indicates some similarity in their preferred food resources, implying possible competition between these two emblematic megaherbivores (Bocherens et al., 1996, 2005, 2011a).

Among all the herbivores, bovid samples yielded the most variable carbon isotopic values, with δ^{13}C and δ^{15}N values respectively ranging from −21.3‰ to −18.9‰ and from +5.5 to +10.5‰ (n = 17). This wide distribution is probably caused by their ecological plasticity and also

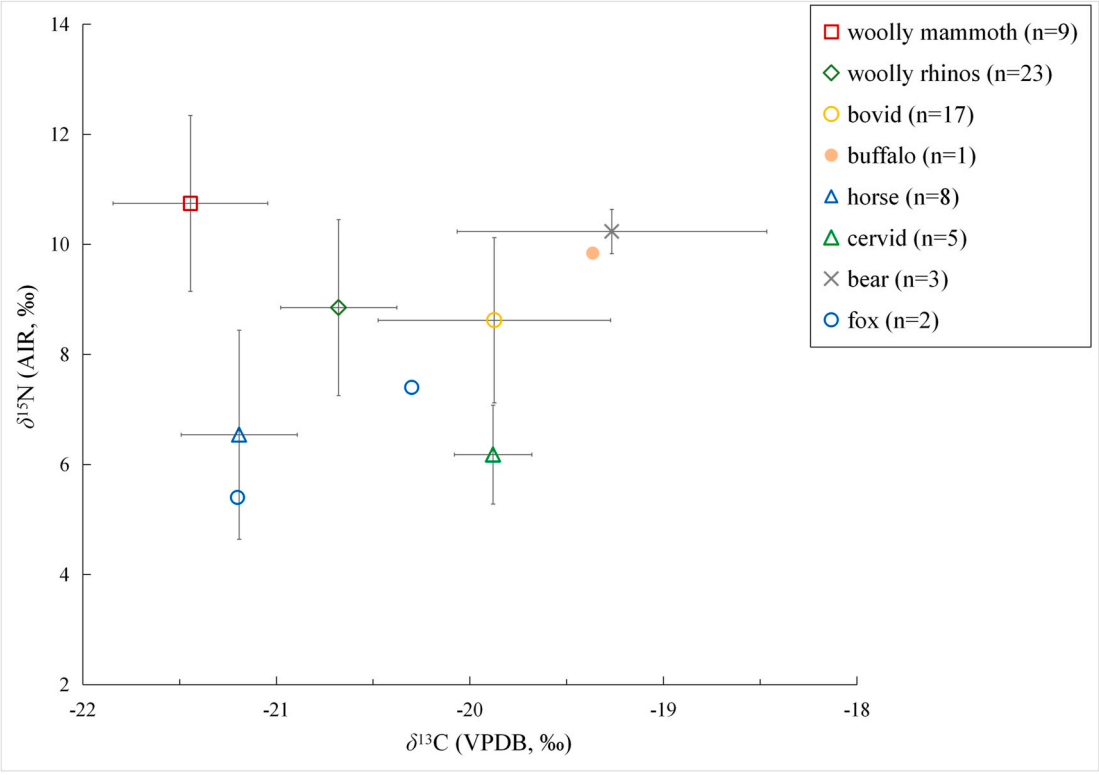

Fig. 3. Mean and standard deviation of δ^{13}C and δ^{15}N values of the *Mammuthus-Coelodonta* Faunal Complex from Yanjiagang and Daqing Museum, Heilongjiang Province, Northeast China.

possibly some level of taxonomic uncertainty in the indentification of the different bovid species (Bocherens, 2015). Nevertheless, when Yanjiagang specimens hereby attributed to *Bison* are considered, they also exhibit a broad isotopic distribution shown in Fig. 2a, possibly associated to the consumption of variable food resources, although their higher $\delta^{15}N$ values indicate substantial grazing behavior, mainly feeding on herbs and grasses/sedges (Bocherens et al., 2015a). Generally, *Bison* is considered as a typical grazer, but emerging evidence has begun to reveal their relatively higher ecological plasticity, a potentially crucial factor underlying their success as important herbivores of the mammoth steppe ecosystem and their eventual survival into the present (Mendoza and Palmqvist, 2008; Feranec et al., 2009; Bocherens et al., 2015a; Davies et al., 2019; Hofman-Kamińska et al., 2019). Interestingly, one *Bubalus* sample identified by ZooMS, had both high $\delta^{13}C$ and $\delta^{15}N$ values of −19.4‰ and +9.8‰, respectively, which probably demonstrates a preference for herbs with higher $\delta^{13}C$ value in open environments. *Bubalus* in tropical archaeological sites also yielded much higher $\delta^{13}C$ values than other sympatric cervids (Tian et al., 2013; Chen et al., 2015), corresponding to their grazing behavior in the areas adjacent to water sources.

Horse samples indicate feeding on the leaves of shrubs or trees, with relatively lower $\delta^{13}C$ (−21.2 ± 0.3‰) and $\delta^{15}N$ values (+6.5 ± 1.9‰, n = 8), suggesting a potential browsing preference (Bocherens et al., 2015a). Late Pleistocene horses have been typically considered as grazers (Schwartz-Narbonne et al., 2019), with their ecological niche inferred from stable isotopes overlapping with that of woolly mammoths in some cases (Drucker et al., 2018; Schwartz-Narbonne et al., 2019). The distinctive ecology of Late Pleistocene horses revealed from isotopes represents their ecological plasticity, which was also seen in their predecessors during the Pliocene and Pleistocene (MacFadden, 1999; Semprebon et al., 2016). The cervids from Daqing Museum samples probably ingested lichen/mosses and leaves, as indicated by the relatively higher $\delta^{13}C$ (−19.9 ± 0.2‰) and lower $\delta^{15}N$ values (+6.2 ± 0.9‰, n = 5) (Fox-Dobbs et al., 2008).

Among our Daqing Museum samples (Ma et al., 2017), two foxes have comparably lower $\delta^{15}N$ values (+7.4‰, +5.4‰), possibly indicative of preying on small mammals, which are known to display lower $\delta^{15}N$ values than those of large herbivores in several cases (e.g. Baumann et al., 2020). The high $\delta^{15}N$ values of brown bear samples (+10.2 ± 0.4‰, n = 3) suggest a carnivorous diet. However, all the herbivores in NE China reflect a relatively high $\delta^{15}N$ baseline. Therefore, considering the ecological plasticity of brown bear from both modern and fossil evidence in different regions, it is still inadequate to assert that brown bear from this region were predominantly carnivorous (Matheus, 1995; Bocherens et al., 2011b; Bojarska and Selva, 2012; García-Vázquez et al., 2018; Rey-Iglesia et al., 2019). Further investigations on $\delta^{15}N$ values of collagen amino acids could provide the chance to decipher the paleoecology of brown bears thoroughly, as it has been successfully done on Romanian cave bear which was found to be herbivorous despite plausibly carnivorous bulk $\delta^{15}N$ values (Naito et al., 2020).

4.1.2. Geographical Society Cave

The paleoecology of the Geographical Society Cave fauna is also characterized by the isotopic specificity of the woolly mammoth, though only one mammoth sample is of very limited explanatory power. However, the enrichment in average $\delta^{15}N$ values between the woolly mammoth and other coexisting herbivores is different from the value observed in China. The analyzed mammoth sample from Geographical Society Cave had a $\delta^{15}N$ value 5.1‰ higher than the average of other herbivores (mammoth $\delta^{15}N$: +9.9‰, n = 1; $\delta^{15}N$ of rhinoceros, bisons, horse, and cervid: +4.8 ± 0.8‰, n = 9); while an enrichment of only 2.5‰ was calculated for the samples from NE China ($\delta^{15}N$ of mammoth: +10.7 ± 1.6‰, n = 9; $\delta^{15}N$ of rhinoceros, bison, horse, and cervid: +8.2 ± 1.8‰, n = 53). A possible explanation here is that the Russian mammoth was sampled from the dentine of DP3/4 from a juvenile individual, whilst the other species were all sampled from bones. The $\delta^{15}N$ values of mammoth dentine (all molars and tusks sampled) are typically 0.7–2.6‰ higher than those of bones (Arppe et al., 2019), while the $\delta^{15}N$ value of mammoth DP3 is 2.2‰ higher than other adult tissues (Metcalfe et al., 2010). Milk consumption by juvenile mammoth is known to span at least 5 years (Rountrey et al., 2007; Cherney, 2016), consequently the DP3/4 formed during the first three years of life is obviously effected by milk intake (Metcalfe et al., 2010). After calculating the projected adult $\delta^{15}N$ for the Geographical Society Cave mammoth by subtracting 2.2‰ (also shown in Fig. 2b), the $\delta^{15}N$ gap between mammoth and other coeval herbivores was also constant approximately 3‰ (Kuitems et al., 2012).

Among other herbivores, one moose yielded a low $\delta^{15}N$ value of +2.9‰, possibly linked to heavy reliance on foliage, which was congruent to the other isotopic evidence elsewhere (Baskin and Danell, 2003; Hobbie et al., 2009; Wam and Hjeljord, 2010; Hofman-Kamińska et al., 2018). On the contrary, the relatively higher $\delta^{15}N$ values of horse, woolly rhinoceros, bison, and wapiti probably reflect the lower proportion of foliage in their diet compared to the moose. The similar isotopic signatures of bisons and wapitis may suggest a feeding preference on herbs or lichen/mosses, while the horse probably consumed a mixture of grasses/sedges and leaves, with the lowest $\delta^{13}C$ values.

Compared to NE China, all the herbivores in Geographical Society Cave had prevalently lower $\delta^{15}N$ values. One possible factor involved here would be regional differences in nitrogen cycling dynamics (Tahmasebi et al., 2018). Moreover, these generally lower $\delta^{15}N$ values in the Geographical Society Cave faunal samples may indicate a somewhat greater browsing component within the dietary composition of the local herbivores overall, implying a different environmental context in this coastal area. This could be supported by paleoenvironmental studies on the southern coastal reaches of the Russian Far East, which revealed a landscape dominated by coniferous forests with shrubs and shrub tundra, as well as partial steppe during the warm period (Tankersley and Kuzmin, 1998).

In sum, even when considering the possible impact of variations in $\delta^{15}N$ baselines and vegetation composition in different environments, the conservative isotopic pattern of all herbivorous faunas still exhibits relatively stable ecological niches of *Mammuthus-Coelodonta* Faunal Complex, though the faunal ecology implies environmental diversity of different subregions in Northeast Asia.

4.2. Paleoecology of the pre-LGM Mammuthus-Coelodonta Faunal Complex at the southeast limit of mammoth steppe

4.2.1. Paleoenvironmental and paleoclimatic background of this region during MIS 3

The AMS ^{14}C dating results of seven mammal bones from Yanjiagang in this study all belonged to MIS 3, the interstadial of the last glacial period (Grootes et al., 1993). Previous published AMS ^{14}C dates from the mammal bones of Geographical Society Cave were also fall into the same stage (Kuzmin et al., 2001; Baryshnikov, 2014). Therefore, the two sites could be reasonably used for a joint discussion on the paleoecology of this fauna during MIS 3 at the southeastern margin of the mammoth steppe in Northeast Asia.

The landscape of Northeast China is characterized by the Northeast Plain, the Quaternary mammal fossils in this region were mainly found in river terraces, lacustrine deposits, bed facies deposits, and valley basin. Multiple palynological studies indicated a landscape covered by *Artemisia*, Asteraceae, Gramineae, Cyperaceae, with a few *Picea*, reflecting the expansion of a cold-dry meadow-steppe environment during the Late Pleistocene in NE China (Heilongjiang Cultural Relics Management Committee, 1987; Jiang et al., 2019; Li et al., 2019a, b). Fossil pollen records in eastern China, Tibetan Plateau, and northwestern China have documented vegetation change during MIS 3 (60–27 ka), though lacking direct palynological sequence in NE China during this stage (Zhao et al., 2014).

From the perspective of paleoclimate, all the evidence from ice cores,

oceanic, and terrestrial deposits indicate that the Earth's climate system experienced a series of rapid changes during MIS 3 on centennial to millennial timescales (Siddall et al., 2008; Harris, 2019). In China, paleoclimatic studies had suggested that MIS 3 was warmer and more humid, with highly frequent climatic changes as a result of the frequent sea level changes, and synergic effects of temperate continental and Pacific warm-wet monsoonal climate in Northeast Asia (Porter and An, 1995; Yao et al., 1997; Zhou et al., 2001; Herzschuh, 2006; Harris, 2019). During the time span of our samples from Yanjiagang (47,763–42,145 yr BP), ice core records from the Guliya ice cap in Tibet reveal high temperature during MIS 3 (58–32 ka) based on oxygen isotopes, but also included at least four cooling events, especially two events occurred between 47 and 43 ka (Yao et al., 1997). The grain size data in Chinese Loess found six Heinrich events corrected with the North Atlantic during the last glacial, one of them occurred in 43.5–42 ka (Porter and An, 1995). The MIS 3 climate of the Salawusu River valley recorded by paleo-mobile dune sands have documented very frequent climatic fluctuations, including at least nine wet-warm and ten cold-dry fluctuations during 58,900–22,300 (Wen et al., 2009).

Geographical Society Cave is located in Southern Siberia, this coastal area was found to be more humid than the Arctic regions over this period (Anderson and Lozhkin, 2015). Meanwhile, the palynological samples in Geographical Society Cave revealed a significant presence of larch-birch forest, a floral assemblage typical of the boreal forest, which probably lead to the lower δ^{15}N values of the herbivores compared to NE China (Tankersley and Kuzmin, 1998). However, at the end of the last glaciation (11–12 ka), judging from the findings in Bliznets Cave situated near Geographical Society Cave, the steppe polecat (*Mustela eversmanii*) and other species of the steppe zone dispersed from Central Asia as far as the Pacific coast (Baryshnikov and Alekseeva, 2017).

In sum, we premised multiple environmental and climatic background in our studied region during MIS 3 to better discuss the paleoecology of this fauna under such climatic oscillations, vegetation changes, and regional geographic differences (Qian and Ricklefs, 2000; Willerslev et al., 2014).

4.2.2. Paleoecology of the pre-LGM Mammuthus-Coelodonta Faunal Complex in NE China

Chinese researchers have concluded that mammoths had two thriving periods in the Late Pleistocene, along with their southward migration waves based on early radiocarbon dating results from the 1980s, which were 34–26 ka and 23–12 ka respectively (Dong et al., 1996; Jin et al., 1998). Hereby, we stress that it is premature to draw upon the precise Late Pleistocene history of the woolly mammoth in NE China based on still insufficient robust radiocarbon dates (Turvey et al., 2013). Despite this uncertainty, our results confirmed that woolly mammoths were thriving in NE China during MIS 3. Notably, the southernmost record of the woolly mammoth globally is situated in Shandong Province, around 36°N and dated to 33,150 ± 250 BP, which places it in one Heinrich cooling event during the warmer MIS 3a stage (Porter and An, 1995; Takahashi et al., 2007).

By contrast, the woolly rhinoceros was apparently more abundant and more widely distributed in China than the woolly mammoth (Tong, 2004; Zhang et al., 2016). Faunistically, woolly rhinoceros not only accompanied woolly mammoths in NE China, but had also been previously identified as sympatric with the straight-tusk elephant *Palaeoloxodon* in warmer zones (Tong, 2004). In England, *Coelodonta-Palaeoloxodon* sympatry is also known from interglacial faunas dated to MIS 7 (Schreve, 2001), Schreve (2019) over a period when woolly rhinoceros in Europe dispersed as far south as the Iberian Peninsula (Álvarez-Lao and García, 2011). The aforementioned foraging flexibility of the woolly rhinoceros could have contributed to its wide breadth of ecological tolerance, allowing woolly rhinoceros to become versatile megaherbivores thriving in both cold and temperate environments. An alternative explanation is that the woolly rhinoceros migrated southward during the cooling epochs. Remarkably, these two alternative hypotheses both contradict previous statements about their lower tolerance to marginal/suboptimal ecological conditions and lower migration ability, which were founded on their narrower geographic range comparing to mammoths and physical similarity with their modern counterparts (Boeskorov, 2001; Stuart and Lister, 2012).

The credible presence of the *Bubalus* at Yanjiagang affords us a chance to explore an inexplicable case of the co-occurrence of *Bubalus* and *Mammuthus-Coelodonta* Faunal Complex from Late Pleistocene Northeast Asia (Tong, 2007). In eastern China, *Bubalus* was widely distributed from north to south throughout the Pleistocene, including six species recognized so far (Xue and Li, 2000; Dong et al., 2014). However, Pleistocene *Bubalus* has never been recovered from the emblematic loess deposits of Northwest China, which are conventionally interpreted as representing a dry and cold environments (Xue and Li, 2000; Tong et al., 2015). In NE China, *B. wansjocki* was the common species that coexisted with the *Mammuthus-Coelodonta* Faunal Complex (Tong, 2007; Tong et al., 2015; Zhang et al., 2019), although this species was also a common element of the *Palaeoloxodon-Coelodonta* Fauna, and was even found in warm temperate Jiangsu Province in the Yangtze River Valley (Xue and Li, 2000). In Europe, only one *Bubalus* species, *B. murrensis,* occurred rarely during the Middle Pleistocene, previously thought to be extinct in Europe after the end of the Eemian (MIS 5e) interglacial (Koenigswald et al., 2019). Astonishingly, *B. murrensis* dated to the Allerød interstadial (ca. 12,800) at the end of the Pleistocene was recently identified at Kolomna near Moscow, Russia (Vislobokova et al., 2020). Modern *Bubalus* are restricted in their native distribution to tropical Asia, and following a uniformitarian interpretation, Pleistocene *Bubalus* had long been conservatively speculated to be ecologically similar to its modern counterparts, inhabiting warm and temperate environments.

The ^{14}C date of the Yanjiagang *Bubalus* was not strictly contemporaneous with the woolly mammoths and woolly rhinoceros at this site. Yet on the other hand, the age of this *Bubalus* (43,447 ± 833 ^{14}C yr BP, 48,823–45,245 cal yr BP) was surprisingly very close to the mammoth recently dated in Zhalai Nur from Inner Monglia (ZLMMXAMS9, 43,500 + 1000/–890 ^{14}C yr BP, 48,800–45,400 cal yr BP, 2σ, measured in Kiel and by Beta Analytic. See in Table 2, Zhang et al., 2019), and thus supporting *Bubalus* as a constituent taxon of the Late Pleistocene *Mammuthus-Coelodonta* Faunal Complex in NE China. During the age range of the Zhalai Nur mammoth and the Yanjiagang *Bubalus*, three climatic phases had been found in Inner Monglia, two cold periods C6 (46,200–44,600yr BP) and C7 (49,500–48,200yr BP), and one warm period W7 (48,200–46,200yr BP) (Wen et al., 2009). Even though it is not realistic to precisely match the age information conducted from different proxies, this study still contributes solid evidence that the *Bubalus* was distributed far north during such frequent climatic oscillations. Considering the cumulative temporal-spatial and ecological evidence of a mixed fauna with woolly mammoth, woolly rhinoceros, and buffalo, frequent shifts in species distribution ranges coincided with climatic oscillations may have played an important role in East Asian faunal perturbations during MIS 3.

China shows a great geological and geographic complexity, with the uplift of the Tibetan Plateau having profoundly influenced the evolution of Chinese landscape, climate, and faunas during the Late Cenozoic (Deng et al., 2019). Traditionally, Quaternary zoogeographic records in China were divided into the Palearctic and Oriental biozones. However, increasing evidence claimed that the bidirectional migration corridor continuously served for faunistic migration and early human dispersal (Norton et al., 2011a; Bae et al., 2017, 2018; He et al., 2017; Yang et al., 2020). Altitudinally, most of central- and eastern China remained less than 1000 m above sea level, so no geographic barrier could prevent the mammal migrations between the north and south in eastern China (Norton et al., 2011b). The fauna from Geographical Society Cave in south Far East Russia was also characterized by a mixture of northern and southern species (Baryshnikov, 2014; 2015a, b; 2016). Therefore, Northeast Asia has been a region under the influence of complex faunal

interchanges between different climatic zones.

Alongside temperature, water availability is another significant abiotic factor that influences the environment's capacity for sustaining large mammals, especially for taxa like *Bubalus*. In eastern China, water resources were abundant due to the precipitation influenced by summer monsoon, especially during the interstadials (Wang et al., 2001; Herzschuh, 2006; Chang et al., 2009). Moreover, large rivers and lakes were documented by widely distributed alluvial-fluvial deposits during the Late Pleistocene (Jin et al., 2016; Wu et al., 2016). Therefore, frequent migrations along river systems seem an amenable scenario for distribution shifts in large mammals during the Pleistocene, especially for taxa like *Bubalus*, which is generally interpreted as favoring mild environments with plentiful supplies of water (Koenigswald et al., 2019). This present study highlights the importance of quantitative paleoecological approaches in reevaluating the interaction between mammalian paleoecology and paleoenvironment from different proxies.

4.2.3. Comparison of mammoth carbon and nitrogen isotopes with other regions

Among all the analyzed species, woolly mammoth appears to have the most conservative dietary habits, so it is interesting to investigate possible regional differences. We compiled hereby carbon and nitrogen isotopes of mammoth bones from the regions of western and eastern Beringia. All the samples dated as pre-LGM (from >45,000 to 24,600 ^{14}C yr BP) were chosen from Asia and Arctic America, as indicated in Fig. 4a (Taymyr Peninsula, Northeastern Siberia mainly includes Bykovsky Peninsula and Yakutia, Alaska and Yukon). As only three Chinese mammoth samples from Yanjiagang are well-dated, we included a further five bone samples from the Daqing Museum collections (Ma et al., 2017) to ensure a comparable sample size. We only selected bone samples to avoid possible weaning effect. All the data are listed in Supplementary Table 3 and generally summarized in Table 3 and plotted in Fig. 4b.

1. Iacumin et al. (2000); 2. Szpak et al. (2010); 3. Iacumin et al. (2010); 4. Arppe et al. (2019); 5. Kuitems and Kolfschoten, 2019; 6. Ma et al. (2017); 7. Metcalfe et al. (2010); 8. Metcalfe (2011); 9. Mann et al. (2013); 10. Schwartz-Narbonne et al. (2019).

The sheer geographical vastness of northern Asia permits comprehensive comparison of woolly mammoth paleoecology with latitudinal controls, a prerequisite not achieved by European samples, even though stable isotopic data for woolly mammoths are most abundant from Europe. Whereas in mid-continental North America, difficulties of discriminating the woolly (*M. primigenius*) and Columbian mammoths (*M. columbi*) due to overlaps in morphology and distribution (notwithstanding genetic introgression: Enk et al., 2016; Widga et al., 2017; Zhang, 2020) present severe obstacles in auditing published stable isotopic data (e.g. in Widga et al., 2020) for our purpose. As shown in Table 3 and Fig. 4, the three Asian subregions all yielded higher δ^{15}N values and lower δ^{13}C values than in eastern Beringia. This phenomenon has been discussed by Szpak et al. (2010), who interpreted it as the result of a generally more arid and cooler environments in Siberia compared to eastern Beringia. However, among all three subregions in Asia, the mammoth from middle-latitude NE China had both higher δ^{13}C and δ^{15}N values than those from Taymyr Peninsula and Northeastern Siberia.

Globally, δ^{15}N values of soil and plants are negatively correlated with mean annual precipitation (MAP) and positively correlated with mean annual temperature (MAT) (Ambrose, 1991; Nadelhoffer et al., 1996; Hartman, 2011). However, multiple complex environmental factors, such as the microbial processing of organic matter and mineral association could also significantly influence the δ^{15}N variability of soil and plants (Craine et al., 2015a, b). It is hard to directly compare the precipitation and temperature of these subregions during the pre-LGM, so we compare the modern climatic data of these subregions to roughly reflect the regional difference. In Supplementary Table 4, we summarize the annual precipitation and average air temperature during the several years from four selected locations belonging to these four subregions discussed here, the data are cited from IAEA-WISER (International Atomic Energy Agency, Water Isotope System for data analysis visualization and Electronic Retrieval). It shows that middle-latitude NE China had the highest annual average temperature with at least ten degree higher than other regions, but no clear relationship was found between precipitation and latitude. Therefore, the highest δ^{15}N values in NE China are possibly more controlled by higher temperature, rather than aridity (Amundson et al., 2003; Craine et al., 2009). Alternatively, this phenomenon might reflect that soil in warmer NE China associate with higher rates of microbial processing of organic matter and greater concentrations of clay, results in a greater proportion of soil ^{15}N, leading to the higher δ^{15}N values of plants (Craine et al., 2015a, b).

On the other hand, the higher δ^{13}C values of the NE China mammoths compared to Arctic regions may also related to higher temperature (Heaton, 1999). Soil carbon isotopes from Late Pleistocene NE China were found to have higher organic δ^{13}C values for the deposits during the interstadial rather than the glacial phrase, consequently temperature probably affected δ^{13}C values of vegetation more than precipitation and atmospheric CO_2 (Lu et al., 2015). Direct carbon isotopes of plants from northern China also show a strong correlation with temperature (Wang et al., 2013). In Western Europe, bioapatite δ^{13}C values of Late Pleistocene mammoth also displayed a geographical difference, where the colder/-more humid northeastern parts of the European study area had lower δ^{13}C values than warmer/drier southwestern parts (Arppe et al., 2011).

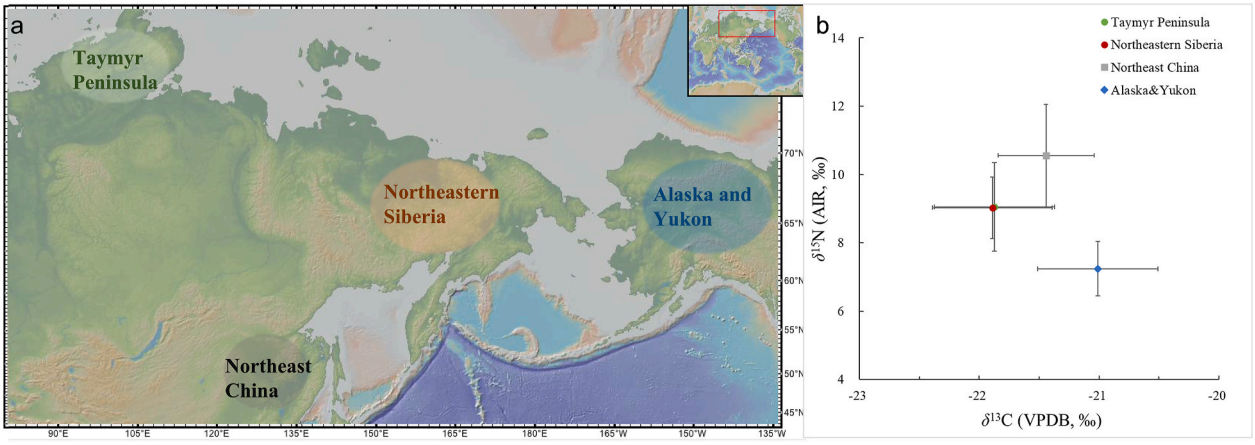

Fig. 4. Comparison of mammoth ecology from Asia and North America during the pre-LGM. a. Map of the regions for comparison; b. carbon and nitrogen stable isotopes of mammoth bones from Taymyr Peninsula, Northeastern Siberia, Northeast Asia, and Alaska & Yukon (Map of Fig. 4a was modified from GeoMapApp www.geomapapp.org; Data resources of Fig. 4b are the same as those in Table 3.).

Table 3
Summary of the mean values and Standard Deviation (SD) of $\delta^{13}C$ and $\delta^{15}N$ values of mammoth bones from Asia and North America during the pre-LGM.

Continent	Subregion	Latitude	Amounts	$\delta^{13}C$	SD	$\delta^{15}N$	SD	References
Asia	Taymyr Peninsula	74°N	15	−21.9	0.5	9.1	1.3	1, 2
	Northeastern Siberia	60–75°N	40	−21.9	0.5	9.0	0.9	1, 2, 3, 4, 5
	Northeast China	40–50°N	8	−21.4	0.4	10.6	1.5	6, this study
America	Alaska &Yukon	60–75°N	25	−21.0	0.5	7.2	0.8	2, 7, 8, 9,10

Therefore, both the higher $\delta^{13}C$ and $\delta^{15}N$ values of mammoth in NE China possibly correlate more with high temperature in these study Asian subregions, which also coincide with the faunal mixture in this mid-latitude region. The identification of more comparable data emerging from North America (resting on future works with the aim to further discern *M. primigenius* and *M. columbi* occurrences in the northern and mid-continent) and other areas from middle-latitude Asia will be useful to deepen the discussion on regional difference within and between each continent.

5. Conclusions

In this study, stable carbon and nitrogen isotopic analyses, ZooMS, and radiocarbon dating were combined to explore the paleoecology of the *Mammuthus-Coelodonta* Faunal Complex in Northeast Asia. In Yanjiagang (NE China) and Geographical Society Cave (Russian Far East), mammoth exhibited the highest $\delta^{15}N$ values and relatively lower $\delta^{13}C$ values in comparison to other large herbivore species of the associated faunas, reflecting their preference for grasses and sedges. The woolly rhinoceros, bison, and horse from our studied samples appear to have high ecological flexibility based on the isotopic signals from different sites. The prevalently lower herbivore $\delta^{15}N$ values at Geographical Society Cave site could be in line with a significant boreal forest component in the associated flora.

Reconciling the stable isotopes, radiocarbon dating, and paleoenvironmental evidence at Yanjiagang, we discuss the co-occurrence of *Mammuthus-Coelodonta* Faunal Complex with the comparably thermophilic *Bubalus* in NE China. This unusual faunal combination coincided with climatic fluctuations in this region during MIS 3, which led to frequent faunal exchanges in eastern China, where vast areas lower than 1000 m above sea level served as the migration corridor for early humans and mammals during the Quaternary. In Northeast Asia, the fauna was susceptible to the synergistic effects of climatic oscillations, multiple climatic systems, and local geographic traits, which probably facilitated more frequent interactions between Palearctic and Oriental faunas, shaping the unique ecological scenario at the southeastern limit of the mammoth steppe biome. Sulfur or strontium isotopic work in the future may provide the potential to directly track the migration of mammals and early humans in East Asia.

When comparing the carbon and nitrogen isotopes of mammoth from middle-high latitude Asia and America, we found that both $\delta^{13}C$ and $\delta^{15}N$ values of NE China are higher than arctic Asia, resulting from the warmer environment of the middle-latitude area. This will be further verified when sufficient data has emerged from the middle latitude region of the Holarctic mammoth steppe. Further research is necessary in this region on all aspects of the *Mammuthus-Coelodonta* Faunal Complex, to capture the completely dynamics of its evolution and extinction.

Declaration of competing interest

The authors declare that they have no known competing financial interests or personal relationships that could have appeared to influence the work reported in this paper.

Acknowledgements

We sincerely appreciate Profs. Huili Yu and Changzhu Jin for supplying research materials. We thank a lot for Profs. Tao Deng, Haowen Tong, and Keliang Zhao from IVPP for their helpful communication and suggestions about this work. In particular, we sincerely appreciate two anonymous reviewers and the editors for their valuable suggestions and patient corrections. We are also grateful for Bing Yi and Quyi Jiang from the University of Chinese Academy of Sciences, and Chris Baumann, Sophia Haller von Hallerstein, and Peter Tung from the University of Tübingen for their assistance with the lab work. This work was supported by the Chinese Academy of Sciences (Grant No. XDB26000000, XDA20070203), the National Natural Science Foundation in China (Grant No. 41773008, No. 42002005, and No. 41872022), Senckenberg Centre for Human Evolution and Palaeoenvironment (S-HEP) in Universität Tübingen, Zoological Institute of the Russian Academy of Sciences in Saint-Petersburg (ZIN RAS) (state research project AAAA-A19-119032590102-7) and the Special Research Assistant Funding of the Chinese Academy of Sciences (1323110005).

Appendix A. Supplementary data

Supplementary data to this article can be found online at https://doi.org/10.1016/j.quaint.2020.12.024.

References

Álvarez-Lao, D.J., García, N., 2011. Southern dispersal and Palaeoecological implications of woolly rhinoceros (*Coelodonta antiquitatis*): review of the Iberian occurrences. Quat. Sci. Rev. 30, 2002–2017.

Ambrose, S.H., 1991. Effects of diet, climate and physiology on nitrogen isotope abundances in terrestrial foodwebs. J. Archaeol. Sci. 18, 293–317.

Amundson, R., Austin, A.T., Schuur, E.A.G., et al., 2003. Global patterns of the isotopic composition of soil and plant nitrogen. Global Biogeochem. Cycles 17, 1031.

Anderson, P.M., Lozhkin, A.V., 2015. Late Quaternary vegetation of Chukotka (northeast Russia), implications for glacial and Holocene environments of Beringia. Quat. Sci. Rev. 107, 112–128.

Arppe, L., Aaris-Sørensen, K., Daugnora, L., et al., 2011. The palaeoenvironmental $\delta^{13}C$ record in European woolly mammoth tooth enamel. Quat. Int. 245, 285–290.

Arppe, L., Karhu, J.A., Vartanyan, S., et al., 2019. Thriving or surviving? The isotopic record of the Wrangel Island woolly mammoth population. Quat. Sci. Rev. 222, 105884.

Bae, C.J., Douka, K., Petraglia, M.D., 2017. On the origin of modern humans: Asian perspectives. Science 358, eaai9067.

Bae, C.J., Li, F., Cheng, L., et al., 2018. Hominin distribution and density patterns in Pleistocene China: climatic influences. Palaeogeogr. Palaeoclimatol. Palaeoecol. 512, 118–131.

Barnosky, A.D., 2004. Assessing the causes of Late Pleistocene extinctions on the continents. Science 306, 70–75.

Baryshnikov, G.F., 2014. Late Pleistocene hyena *Crocuta ultima ussurica* (Mammalia: Carnivora: Hyaenidae) from the Paleolithic site in geographical society cave in the Russian Far East. Proceedings of the Zoological Institute RAS 318, 197–225.

Baryshnikov, G.F., 2015a. Late Pleistocene Canidae remains from geographical society cave in the Russian Far East. Russ. J. Theriol. 14, 65–83.

Baryshnikov, G.F., 2015b. Late Pleistocene Ursidae and Mustelidae remains (Mammalia, Carnivora) from geographical society cave in the Russian Far East. Proceedings of the Zoological Institute RAS 319, 3–22.

Baryshnikov, G.F., 2016. Late Pleistocene Felidae remains (Mammalia, Carnivora) from geographical society cave in the Russian Far East. Proceedings of the Zoological Institute RAS 320, 84–120.

Baryshnikov, G.F., Alekseeva, E.V., 2017. Late Pleistocene and Holocene *Mustela* remains (Carnivora, Mustelidae) from Bliznets cave in the Russian Far East. Russ. J. Theriol. 16, 1–14.

Baskin, L., Danell, K., 2003. Moose-*Alces alces*. In: Baskin, L., Danell, K. (Eds.), Ecology of Ungulates A Handbook of Species in Eastern Europe and Northern and Central Asia. Springer-Verlag Berlin Heidelberg, Berlin, pp. 91–108.

Baumann, C., Starkovich, B.M., Drucker, D.G., et al., 2020. Dietary niche partitioning among Magdalenian canids in southwestern Germany and Switzerland. Quat. Sci. Rev. 227, 106032.

Bocherens, H., 2002. Preservation of isotopic signals (^{13}C, ^{15}N) in Pleistocene mammals. In: Ambrose, S.H., Katzenberg, M.A. (Eds.), Biogeochemical Approaches to Paleodietary Analysis. Kluwer Academic Publishers, Boston, pp. 65–88.

Bocherens, H., 2003. Isotopic biogeochemistry and the paleoecology of the mammoth steppe fauna. In: Reumer, W.F., Braber, F., Mol, D., et al. (Eds.), Advances in Mammoth Research, pp. 57–76. Rotterdam, Deinsea.

Bocherens, H., 2015. Isotopic tracking of large carnivore palaeoecology in the mammoth steppe. Quat. Sci. Rev. 117, 42–71.

Bocherens, H., Fizet, M., Mariotti, A., et al., 1991. Isotopic biogeochemistry (^{13}C, ^{15}N) of fossil vertebrate collagen: application to the study of a past food web including Neandertal man. J. Hum. Evol. 20, 481–492.

Bocherens, H., Fizet, M., Mariotti, A., et al., 1994. Contribution of isotopic biogeochemistry (^{13}C, ^{15}N, ^{18}O) to the paleoecology of mammoths (*Mammuthus primigenius*). Hist. Biol. 7, 187–202.

Bocherens, H., Pacaud, G., Lazarev, P.A., et al., 1996. Stable isotope abundances (^{13}C, ^{15}N) in collagen and soft tissues from Pleistocene mammals from Yakutia: implications for the palaeobiology of the Mammoth Steppe. Palaeogeogr. Palaeoclimatol. Palaeoecol. 126, 31–44.

Bocherens, H., Billiou, D., Patou-Mathis, M., et al., 1997. Paleobiological implications of the isotopic signatures (^{13}C, ^{15}N) of fossil mammal collagen in Scladina Cave (Sclayn, Belgium). Quat. Res. 48, 370–380.

Bocherens, H., Drucker, D.G., Billiou, D., et al., 2005. Isotopic evidence for diet and subsistence pattern of the Saint-Césaire I Neanderthal: review and use of a multi-source mixing model. J. Hum. Evol. 49, 71–87.

Bocherens, H., Drucker, D.G., Bonjean, D., et al., 2011a. Isotopic evidence for dietary ecology of cave lion (*Panthera spelaea*) in North-Western Europe: prey choice, competition and implications for extinction. Quat. Int. 245, 249–261.

Bocherens, H., Stiller, M., Hobson, K.A., et al., 2011b. Niche partitioning between two sympatric genetically distinct cave bears (*Ursus spelaeus* and *Ursus ingressus*) and brown bear (*Ursus arctos*) from Austria: isotopic evidence from fossil bones. Quat. Int. 245, 238–248.

Bocherens, H., Hofmankamińska, E., Drucker, D.G., et al., 2015a. European bison as a refugee species? Evidence from isotopic data on Early Holocene bison and other large herbivores in northern Europe. PloS One 10, e0115090.

Bocherens, H., Drucker, D.G., Germonpré, M., et al., 2015b. Reconstruction of the Gravettian food-web at Předmostí I using multi-isotopic tracking (^{13}C, ^{15}N, ^{34}S) of bone collagen. Quat. Int. 359–360, 211–228.

Boeskorov, G., 2001. Woolly rhino (*Coelodonta antiquitatis*) distribution in Northeast Asia. Deinsea 8, 15–20.

Boeskorov, G.G., Bakulina, N.T., Davydov, S.P., et al., 2011a. Study of pollen and spores from the stomach of a fossil woolly rhinoceros found in the lower reaches of the Kolyma river. Dokl. Biol. Sci. 436, 23–25.

Boeskorov, G.G., Lazarev, P.A., Sher, A.V., et al., 2011b. Woolly rhino discovery in the lower Kolyma River. Quat. Sci. Rev. 30, 2262–2272.

Bojarska, K., Selva, N., 2012. Spatial patterns in brown bear *Ursus arctos* diet: the role of geographical and environmental factors: biogeographical variation in brown bear diet. Mamm Rev. 42, 120–143.

Bronk Ramsey, C., 2017. Methods for summarizing radiocarbon datasets. Radiocarbon 59, 1809–1833.

Bronk Ramsey, C., Higham, T., Bowles, A., et al., 2004. Improvements to the pretreatment of bone at Oxford. Radiocarbon 46, 155–163.

Buckley, M., Collins, M., Thomas-Oates, J., et al., 2009. Species identification by analysis of bone collagen using matrix-assisted laser desorption/ionisation time-of-flight mass spectrometry. Rapid Commun. Mass Spectrom. 23, 3843–3854.

Chang, Y.P., Chen, M.T., Yokoyama, Y., et al., 2009. Monsoon hydrography and productivity changes in the East China Sea during the past 100,000 years: Okinawa Trough evidence (MD012404). Paleoceanography 24, PA3208.

Chen, J., Yin, Y.Q., Li, T., et al., 2016. The *mammuthus-Coelodonta* fauna from Dabusu national key fossil locality, Jilin province. Geol. Bull. China 6, 872–878 (in Chinese with English abstract).

Chen, X., Luo, Y., Hu, Y., et al., 2015. The analysis of the stable carbon and nitrogen isotope of pig offering in a tomb at Qinglongquan Site. Jianghan Archaeology 5, 107–115 (in Chinese with English abstract).

Cherney, M.D., 2016. Records of Growth and Weaning in Fossil Proboscidean Tusks as Tests of Pleistocene Extinction Mechanisms. Doctoral Dissertation. University of Michigan, Michigan.

Craine, J.M., Elmore, A.J., Aidar, M.P.M., et al., 2009. Global patterns of foliar nitrogen isotopes and their relationships with climate, mycorrhizal fungi, foliar nutrient concentrations, and nitrogen availability. New Phytol. 183, 980–992.

Craine, J.M., Brookshire, E.N.J., Cramer, M.D., et al., 2015a. Ecological interpretations of nitrogen isotope ratios of terrestrial plants and soils. Plant Soil 396, 1–26.

Craine, J.M., Elmore, A.J., Wang, L., et al., 2015b. Convergence of soil nitrogen isotopes across global climate gradients. Sci. Rep. 5, 8280.

Davies, G., McCann, B., Sturdevant, J., et al., 2019. Isotopic paleoecology of northern great plains bison during the Holocene. Sci. Rep. 9, 16637.

Deng, T., Wu, F., Zhou, Z., et al., 2019. Tibetan Plateau: an evolutionary junction for the history of modern biodiversity. Sci. China Earth Sci. 63, 172–187.

DeNiro, M.J., 1985. Postmortem preservation and alteration of *in vivo* bone collagen isotope ratios in relation to palaeodietary reconstruction. Nature 317, 806–809.

Dong, W., Xu, Q., Jin, C., et al., 1996. The evolution of Quaternary large herbivores from Northeast China and its relationship with paleoclimatical variation. Vertebr. Pal Asiat. 34, 58–70 (in Chinese with English abstract).

Dong, W., Liu, J., Zhang, L., et al., 2014. The Early Pleistocene water buffalo associated with *Gigantopithecus* from Chongzuo in southern China. Quat. Int. 354, 86–93.

Drucker, D.G., Bocherens, H., Péan, S., 2014. Isotopes stables (^{13}C, ^{15}N) du collagène des mammouths de Mezhyrich (Epigravettien, Ukraine) : implications paléoécologiques. L'Anthropologie 118, 504–517 (in French with English abstract).

Drucker, D.G., Stevens, R.E., Germonpré, M., et al., 2018. Collagen stable isotopes provide insights into the end of the mammoth steppe in the central East European plains during the Epigravettian. Quat. Res. 90, 457–469.

Enk, J., Devault, A., Widga, C., et al., 2016. *Mammuthus* population dynamics in late Pleistocene North America: Divergence, phylogeography, and introgression. Frontiers in Ecology and Evolution 4, 42.

Fellows Yates, J.A., Drucker, D.G., Reiter, E., et al., 2017. Central European woolly mammoth population dynamics: insights from Late Pleistocene mitochondrial genomes. Sci. Rep. 7, 1–10.

Feranec, R.S., Hadly, E.A., Paytan, A., 2009. Stable isotopes reveal seasonal competition for resources between late Pleistocene bison (*Bison*) and horse (*Equus*) from Rancho La Brea, southern California. Palaeogeogr. Palaeoclimatol. Palaeoecol. 271, 153–160.

Fisher, D.C., 2018. Paleobiology of Pleistocene proboscideans. Annu. Rev. Earth Planet Sci. 46, 229–260.

Fox-Dobbs, K., Leonard, J.A., Koch, P.L., 2008. Pleistocene megafauna from eastern Beringia: paleoecological and paleoenvironmental interpretations of stable carbon and nitrogen isotope and radiocarbon records. Palaeogeogr. Palaeoclimatol. Palaeoecol. 261, 30–46.

García-Vázquez, A., Pinto-Llona, A.C., Grandal-d'Anglade, A., 2018. Brown bear (*Ursus arctos* L.) palaeoecology and diet in the Late Pleistocene and Holocene of the NW of the Iberian Peninsula: a study on stable isotopes. Quat. Int. 481, 42–51.

Grootes, P.M., Stuiver, M., White, J.W.C., et al., 1993. Comparison of oxygen isotope records from the GISP2 and GRIP Greenlandice cores. Nature 366, 552–554.

Guthrie, R.D., 1982. Mammals of the mammoth steppe as paleoenvironmental indicators. In: Hopkins, D.M., Matthews, J.V., Schweger, C.E., et al. (Eds.), Paleoecology of Beringia. Academic Press, New York, pp. 307–326.

Guthrie, R.D., 2001. Origin and causes of the mammoth steppe: a story of cloud cover, woolly mammal tooth pits, buckles, and inside-out Beringia. Quat. Sci. Rev. 20, 549–574.

Guthrie, R.D., 2013. Frozen Fauna of the Mammoth Steppe: the Story of Blue Babe. University of Chicago Press, Chicago.

Harris, S., 2019. The relationship of sea level changes to climatic change in northeast Asia and northern North America during the last 75 ka B.P. AIMS Environmental Science 6, 14–40.

Hartman, G., 2011. Are elevated $\delta^{15}N$ values in herbivores in hot and arid environments caused by diet or animal physiology? Funct. Ecol. 25, 122–131.

He, J., Kreft, H., Gao, E., et al., 2017. Patterns and drivers of zoogeographical regions of terrestrial vertebrates in China. J. Biogeogr. 44, 1172–1184.

Heaton, T.H., 1999. Spatial, species, and temporal variations in the $^{13}C/^{12}C$ ratios of C_3 plants: implications for palaeodiet studies. J. Archaeol. Sci. 26, 637–649.

Heilongjiang Cultural Relics Management Committee, 1987. A Late Paleolithic Campsite in Harbin, Heilongjiang. Cultural Relics Press, Beijing (in Chinese with English abstract).

Herzschuh, U., 2006. Palaeo-moisture evolution in monsoonal Central Asia during the last 50,000 years. Quat. Sci. Rev. 25, 163–178.

Higham, T.F.G., Jacobi, R.M., Ramsey, C.B., 2006. AMS Radiocarbon dating of ancient bone using ultrafiltration. Radiocarbon 48, 179–195.

Hobbie, J.E., Hobbie, E.A., Drossman, H., et al., 2009. Mycorrhizal fungi supply nitrogen to host plants in Arctic tundra and boreal forests: ^{15}N is the key signal. Can. J. Microbiol. 55, 84–94.

Hofman-Kamińska, E., Bocherens, H., Borowik, T., et al., 2018. Stable isotope signatures of large herbivore foraging habitats across Europe. PloS One 13, e0190723.

Hofman-Kamińska, E., Bocherens, H., Drucker, D.G., et al., 2019. Adapt or die—response of large herbivores to environmental changes in Europe during the Holocene. Global Change Biol. 25, 2915–2930.

Huang, K., 2008. A preliminary study of the circular heaps of animal bones on the Yanjiagang Site in Harbin. Acta Archaeologica Sinica 1, 1–14 (in Chinese with English abstract).

Iacumin, P., Bocherens, H., Mariotti, A., et al., 1996. An isotopic palaeoenvironmental study of human skeletal remains from the Nile Valley. Palaeogeogr. Palaeoclimatol. Palaeoecol. 126, 15–30.

Iacumin, P., Nikolaev, V., Ramigni, M., 2000. C and N stable isotope measurements on Eurasian fossil mammals, 40 000 to 10 000 years BP: herbivore physiologies and palaeoenvironmental reconstruction. Palaeogeogr. Palaeoclimatol. Palaeoecol. 163, 33–47.

Iacumin, P., Di Matteo, A., Nikolaev, V., et al., 2010. Climate information from C, N and O stable isotope analyses of mammoth bones from northern Siberia. Quat. Int. 212, 206–212.

Ives, J.W., Yang, Z., Beaudoin, A.B., et al., 1994. Human presence in Heilongjiang, China, along the late Pleistocene periphery of Beringia. Curr. Res. Pleistocene 11, 136–138.

Jiang, H.T., Zhao, K.L., Wang, Y., et al., 2019. The survival environment of *mammuthus-Coelodonta* fauna in Qinggang, Heilongjiang province, northeast China. Acta Anthropol. Sin. 38, 148–156 (in Chinese with English abstract).

Jin, C., Xu, Q., Zheng, J., 1998. On the dispersal events of *mammuthus* during the late Late Pleistocene. Vertebr. Palasiat. 36, 47–53 (in Chinese with English abstract).

Jin, H., Xiao, L., Dong, L., et al., 2016. Evolution of permafrost in Northeast China since the late Pleistocene. Sciences in Cold and Arid Regions 8, 269–296.

Kahlke, R.D., 1999. The History of the Origin, Evolution and Dispersal of the Late Pleistocene Mammuthus-Coelodonta Faunal Complex in Eurasia (Large Mammals). Fenske Companies., Rapid City.
Kahlke, R.D., 2014. The origin of Eurasian mammoth faunas (*Mammuthus–Coelodonta* faunal complex). Quat. Sci. Rev. 96, 32–49.
Kirby, D.P., Buckley, M., Promise, E., et al., 2013. Identification of collagen-based materials in cultural heritage. Analyst 138, 4849–4858.
Kirillova, I.V., Argant, J., Lapteva, E.G., et al., 2016. The diet and environment of mammoths in North-East Russia reconstructed from the contents of their feces. Quat. Int. 406, 147–161.
Koenigswald, W., Schwermann, A.H., Keiter, M., et al., 2019. First evidence of Pleistocene *Bubalus murrensis* in France and the stratigraphic occurrences of *Bubalus* in Europe. Quat. Int. 522, 85–93.
Kosintsev, P.A., Lapteva, E.G., Trofimova, S.S., et al., 2012. Environmental reconstruction inferred from the intestinal contents of the Yamal baby mammoth Lyuba (*Mammuthus primigenius* Blumenbach, 1799). Quat. Int. 255, 231–238.
Kuitems, M., Kolfschoten, T. van, van der Plicht, J., 2012. Elevated δ^{15}N values in mammoths: a comparison with modern elephants. Archaeological and Anthropological Sciences 7, 289–295.
Kuitems, M., Kolfschoten, T. van, Tikhonov, A.N., et al., 2019. Woolly mammoth δ^{13}C and δ^{15}N values remained amazingly stable throughout the last ~50,000 years in north-eastern Siberia. Quat. Int. 500, 120–127.
Kuzmin, Y.V., Baryshnikov, G.F., Jull, A.J.T., et al., 2001. Radiocarbon chronology of the Pleistocene fauna from geographic society cave, Primorye (Russian Far East). Curr. Res. Pleistocene 18, 106–108.
Li, Q., Wu, H., Yu, Y., et al., 2019a. Large-scale vegetation history in China and its response to climate change since the Last Glacial Maximum. Quat. Int. 500, 108–119.
Li, X., Zhao, C., Zhou, X., 2019b. Vegetation pattern of northeast China during the special periods since the last glacial Maximum. Sci. China Earth Sci. 62, 1224–1240.
Lister, A.M., Sher, A.V., 2001. The origin and evolution of the woolly mammoth. Science 294, 1094–1097.
Lister, A.M., Sher, A.V., 2015. Evolution and dispersal of mammoths across the northern hemisphere. Science 350, 805–809.
Liu, T.S., Li, X.G., 1984. Mammoths in China. In: Martin, P.S. (Ed.), Quaternary Extinctions. Arizona, University of Arizona Press, pp. 517–527.
Lu, H.Y., Zhang, H.Y., Zeng, L., et al., 2015. Temperature forced vegetation variations in glacial-interglacial cycles in Northeastern China revealed by loess-paleosol deposit. Quat. Sci. 35, 828–836 (in Chinese with English abstract).
Ma, J., Zhang, F.L., Wang, Y., et al., 2017. Tracking the foraging behavior of *Mammuthus primigenius* from the Late Pleistocene of northeast China, using stable isotope analysis. Quat. Sci. 37, 885–894 (in Chinese with English abstract).
MacDonald, G.M., Beilman, D.W., Kuzmin, Y.V., et al., 2012. Pattern of extinction of the woolly mammoth in Beringia. Nat. Commun. 3, 893.
MacFadden, B.J., 1999. Ancient diets, ecology, and extinction of 5-million-year-old horses from Florida. Science 283, 824–827.
Mann, D.H., Groves, P., Kunz, M.L., et al., 2013. Ice-age megafauna in Arctic Alaska: extinction, invasion, survival. Quat. Sci. Rev. 70, 91–108.
Matheus, P.E., 1995. Diet and co-ecology of Pleistocene short-faced bears and brown bears in eastern Beringia. Quat. Res. 44, 447–453.
Mendoza, M., Palmqvist, P., 2008. Hypsodonty in ungulates: an adaptation for grass consumption or for foraging in open habitat? J. Zool. 274, 134–142.
Metcalfe, J.Z., Longstaffe, F.J., Zazula, G.D., 2010. Nursing, weaning, and tooth development in woolly mammoths from Old Crow, Yukon, Canada: implications for Pleistocene extinctions. Palaeogeogr. Palaeoclimatol. Palaeoecol. 298, 257–270.
Metcalfe, J.Z., 2011. Late Pleistocene climate and proboscidean paleoecology in North America: insights from stable isotope compositions of skeletal remains. Doctoral Dissertation. The University of Western Ontario, Canada.
Metcalfe, J.Z., Longstaffe, F.J., Hodgins, G., 2013. Proboscideans and paleoenvironments of the Pleistocene Great Lakes: landscape, vegetation, and stable isotopes. Quat. Sci. Rev. 76, 102–113.
Nadelhoffer, K., Shaver, G., Fry, B., et al., 1996. ^{15}N natural abundances and N use by tundra plants. Oecologia 107, 386–394.
Naito, Y.I., Chikaraishi, Y., Drucker, D.G., et al., 2016. Ecological niche of Neanderthals from Spy Cave revealed by nitrogen isotopes of individual amino acids in collagen. J. Hum. Evol. 93, 82–90.
Naito, Y.I., Meleg, I.N., Robu, M., et al., 2020. Heavy reliance on plants for Romanian cave bears evidenced by amino acid nitrogen isotope analysis. Sci. Rep. 10, 6612.
Norton, C.J., Gao, X., Liu, W., et al., 2011a. Central-East China—A Plio-Pleistocene dispersal corridor: the current state of evidence for Hominin occupations. In: Norton, C.J., Braun, D.R. (Eds.), Asian Paleoanthropology, Vertebrate Paleobiology and Paleoanthropology. Springer Netherlands, Dordrecht, pp. 159–168.
Norton, C.J., Jin, C., Wang, Y., et al., 2011b. Rethinking the Palearctic-Oriental biogeographic boundary in Quaternary China. In: Norton, C.J., Braun, D.R. (Eds.), Asian Paleoanthropology. Springer Netherlands, Dordrecht, pp. 81–100.
Ovodov, N.D., 1977. Late Quaternary fauna of mammals (Mammalia) in south of Ussuri region. In: Yudin, B.S. (Ed.), Fauna and Systematic of Siberian Vertebrates. Nauka, Novosibirsk, Russia, pp. 157–177 (in Russian).
Owen-Smith, N., 1987. Pleistocene extinctions: the pivotal role of megaherbivores. Paleobiology 13, 351–362.
Porter, S.C., An, Z., 1995. Correlation between climate events in the North Atlantic and China during the last glaciation. Nature 375, 305–308.
Pushkina, D., Bocherens, H., Ziegler, R., 2014. Unexpected palaeoecological features of the Middle and Late Pleistocene large herbivores in southwestern Germany revealed by stable isotopic abundances in tooth enamel. Quat. Int. 339–340, 164–178.
Qian, H., Ricklefs, R.E., 2000. Large-scale processes and the Asian bias in species diversity of temperate plants. Nature 407, 180–182.
Reimer, P.J., Austin, W.E.N., Bard, E., et al., 2020. The intcal20 northern hemisphere radiocarbon age calibration curve (0–55 cal kBP). Radiocarbon 62, 725–757.
Rey-Iglesia, A., García-Vázquez, A., Treadaway, E.C., et al., 2019. Evolutionary history and palaeoecology of brown bear in North-East Siberia re-examined using ancient DNA and stable isotopes from skeletal remains. Sci. Rep. 9, 4462.
Rivals, F., Álvarez-Lao, D.J., 2018. Ungulate dietary traits and plasticity in zones of ecological transition inferred from late Pleistocene assemblages at Jou Puerta and Rexidora in the Cantabrian Region of northern Spain. Palaeogeogr. Palaeoclimatol. Palaeoecol. 499, 123–130.
Rivals, F., Lister, A.M., 2016. Dietary flexibility and niche partitioning of large herbivores through the Pleistocene of Britain. Quat. Sci. Rev. 146, 116–133.
Rivals, F., Mihlbachler, M.C., Solounias, N., et al., 2010. Palaeoecology of the Mammoth Steppe fauna from the late Pleistocene of the North Sea and Alaska: separating species preferences from geographic influence in paleoecological dental wear analysis. Palaeogeogr. Palaeoclimatol. Palaeoecol. 286, 42–54.
Rivals, F., Semprebon, G.M., Lister, A.M., 2019. Feeding traits and dietary variation in Pleistocene proboscideans: a tooth microwear review. Quat. Sci. Rev. 219, 145–153.
Rountrey, A.N., Fisher, D.C., Vartanyan, S., et al., 2007. Carbon and nitrogen isotope analyses of a juvenile woolly mammoth tusk: evidence of weaning. Quat. Int. 169–170, 166–173.
Saarinen, J., Eronen, J., Fortelius, M., et al., 2016. Patterns of diet and body mass of large ungulates from the Pleistocene of Western Europe, and their relation to vegetation. Palaeontol. Electron. 19, 1–58.
Saarinen, J., Lister, A.M., 2016. Dental mesowear reflects local vegetation and niche separation in Pleistocene proboscideans from Britain. J. Quat. Sci. 31, 799–808.
Schwartz-Narbonne, R., Longstaffe, F.J., Metcalfe, J.Z., et al., 2015. Solving the woolly mammoth conundrum: amino acid ^{15}N-enrichment suggests a distinct forage or habitat. Sci. Rep. 5, 9791.
Schwartz-Narbonne, R., Longstaffe, F.J., Kardynal, K.J., et al., 2019. Reframing the mammoth steppe: insights from analysis of isotopic niches. Quat. Sci. Rev. 215, 1–21.
Schreve, D.C., 2001. Differentiation of the British late Middle Pleistocene interglacials: the evidence from mammalian biostratigraphy. Quat. Sci. Rev. 20, 1693–1705.
Schreve, D.C., 2019. All is flux: the predictive power of fluctuating Quaternary mammalian faunal-climate scenarios. Philosophical Transactions of the Royal Society B 374, 20190213.
Semprebon, G.M., Rivals, F., Solounias, N., et al., 2016. Paleodietary reconstruction of fossil horses from the Eocene through Pleistocene of north America. Palaeogeogr. Palaeoclimatol. Palaeoecol. 442, 110–127.
Siddall, M., Rohling, E.J., Thompson, W.G., et al., 2008. Marine isotope stage 3 sea level fluctuations: data synthesis and new outlook. Rev. Geophys. 46, RG4003.
Strohalm, M., Hassman, M., Košata, B., et al., 2008. *mMass* data miner: an open source alternative for mass spectrometric data analysis. Rapid Commun. Mass Spectrom. 22, 905–908.
Stuart, A.J., 2015. Late Quaternary megafaunal extinctions on the continents: a short review: late Quaternary megafaunal extinctions. Geol. J. 50, 338–363.
Stuart, A.J., Lister, A.M., 2012. Extinction chronology of the woolly rhinoceros *Coelodonta antiquitatis* in the context of late Quaternary megafaunal extinctions in northern Eurasia. Quat. Sci. Rev. 51, 1–17.
Szpak, P., Gröcke, D.R., Debruyne, R., et al., 2010. Regional differences in bone collagen δ^{13}C and δ^{15}N of Pleistocene mammoths: implications for paleoecology of the mammoth steppe. Palaeogeogr. Palaeoclimatol. Palaeoecol. 286, 88–96.
Tahmasebi, F., Longstaffe, F.J., Zazula, G., 2018. Nitrogen isotopes suggest a change in nitrogen dynamics between the Late Pleistocene and modern time in Yukon, Canada. PloS One 13, e0192713.
Takahashi, K., Wei, G., Uno, H., et al., 2007. AMS ^{14}C chronology of the world's southernmost woolly mammoth (*Mammuthus primigenius* Blum.). Quat. Sci. Rev. 26, 954–957.
Tang, Z.W., Liu, S.H., Lin, Z.R., et al., 2003. The late Pleistocene fauna from Dabusu of Qian'an in Jilin province of China. Vertebr. Palasiat. 41, 145–153 (in Chinese with English abstract).
Tankersley, K.B., Kuzmin, Y.V., 1998. Patterns of culture change in eastern Siberia during the Pleistocene–Holocene transition. Quat. Int. 49, 129–139.
Tian, X., Zhu, C., Shui, T., et al., 2013. Diets, eco-environments and seasonal variations recorded in the oxygen and carbon isotopic compositions of mammal tooth enamel from the Shunshanji site, Sihong County, Jiangsu Province, China. Chin. Sci. Bull. 58, 3788–3795 (in Chinese with English abstract).
Tiunov, A.V., Kirillova, I.V., 2010. Stable isotope (^{13}C/^{12}C and ^{15}N/^{14}N) composition of the woolly rhinoceros *Coelodonta antiquitatis* horn suggests seasonal changes in the diet. Rapid Commun. Mass Spectrom. 24, 3146–3150.
Tong, H.W., 2004. Paleoenvironmental Significance of *Coelodonta* in Different Fossil Assembledges 306–314 (in Chinese with English abstract).
Tong, H.W., 2007. Occurrences of warm-adapted mammals in north China over the Quaternary Period and their paleo-environmental significance. Sci. China Earth Sci. 50, 1327–1340 (in Chinese with English abstract).
Tong, H.W., Patou-Mathis, M., 2003. Mammoth and other proboscideans in China during the late Pleistocene. Deinsea 9, 421–428.
Tong, H.W., Chen, X., Wang, X., 2015. On the skull of *Bubalus youngi* of Late Pleistocene from the plain area of Beijing, China. Quat. Sci. 35, 561–572 (in Chinese with English abstract).
Turvey, S.T., Tong, H., Stuart, A.J., et al., 2013. Holocene survival of Late Pleistocene megafauna in China: a critical review of the evidence. Quat. Sci. Rev. 76, 156–166.
Ukraintseva, V.V., 2013. Mammoths and the Environment. Cambridge University Press, Cambridge.

van der Plicht, J., Palstra, S.W.L., 2016. Radiocarbon and mammoth bones: what's in a date. Quat. Int. 406, 246–251.
van Geel, B., Aptroot, A., Baittinger, C., et al., 2008. The Ecological implications of a Yakutian mammoth's last meal. Quat. Res. 69, 361–376.
van Klinken, G.J., 1999. Bone collagen quality indicators for palaeodietary and radiocarbon measurements. J. Archaeol. Sci. 26, 687–695.
Vereshchagin, N.K., Baryshnikov, G.F., 1982. Paleoecology of the mammoth fauna in the Eurasian arctic. In: Hopkins, D.M., Matthews, J.V., Schweger, C.E., et al. (Eds.), Paleoecology of Beringia. Academic Press, New York, pp. 267–279.
Vereshchagin, N.K., Baryshnikov, G.F., 1991. The ecological structure of the" mammoth fauna" in Eurasia. Ann. Zool. Fenn. 28, 253–259.
Vislobokova, I.A., Tarasenko, K.K., Lopatin, A.A.V., 2020. First discovery of the European buffalo *Bubalus murrensis* (Artiodactyla, Bovidae) from the Pleistocene of the Russian plain. Dokl. Biol. Sci. 491, 125–129.
Wam, H.K., Hjeljord, O., 2010. Moose summer and winter diets along a large scale gradient of forage availability in southern Norway. Eur. J. Wildl. Res. 56, 745–755.
Wang, G.A., Li, J., Liu, X., et al., 2013. Variations in carbon isotope ratios of plants across a temperature gradient along the 400 mm isoline of mean annual precipitation in north China and their relevance to paleovegetation reconstruction. Quat. Sci. Rev. 63, 83–90.
Wang, Y.J., Cheng, H., Edwards, R.L., et al., 2001. A high-resolution absolute-dated late Pleistocene monsoon record from Hulu Cave, China. Science 294, 2345–2348.
Wei, Y., Chen, S.Q., Gao, X., 2012. Re-evaluating the nature of semicirclar structures at the Yanjiagang Site. Acta Anthropol. Sin. 31, 238–249 (in Chinese with English abstract).
Welker, F., Hajdinjak, M., Talamo, S., et al., 2016. Palaeoproteomic evidence identifies archaic hominins associated with the Châtelperronian at the Grotte du Renne. Proc. Natl. Acad. Sci. Unit. States Am. 113, 11162–11167.
Wen, X., Li, B., Zheng, Y., et al., 2009. Climate variability in the Salawusu River valley of the Ordos plateau (Inner Mongolia, China) during marine isotope stage 3. J. Quat. Sci. 24, 61–74.
Widga, C., Lengyel, S.N., Saunders, J., et al., 2017. Late Pleistocene proboscidean population dynamics in the north American Midcontinent. Boreas 46, 772–782.
Widga, C., Hodgins, G., Kolis, K., et al., 2020. Multi-scalar approaches to the stable isotope ecology of late Quaternary proboscideans in the Midcontinent. bioRxiv. https://doi.org/10.1101/2020.01.08.896647.
Willerslev, E., Davison, J., Moora, M., et al., 2014. Fifty thousand years of Arctic vegetation and megafaunal diet. Nature 506, 47–51.
Wu, J., Liu, Q., Wang, L., et al., 2016. Vegetation and climate change during the last deglaciation in the great Khingan mountain, northeastern China. PloS One 11, e0146261.
Xue, X.X., Li, X.C., 2000. Fossil *Bubalus* from Shaanxi, distribution and phylogeny of fossil Bubalus in China. Vertebr. Palasiat. 38, 226–234 (in Chinese with English abstract).
Yang, S.X., Yue, J.P., Zhou, X., et al., 2020. Hominin site distributions and behaviours across the Mid-Pleistocene climate transition in China. Quat. Sci. Rev. 248, 106614.
Yao, T.D., Thompson, L.G., Shi, Y.F., et al., 1997. Climate variation since the Last Interglaciation recorded in the Guliya ice core. Sci. China Earth Sci. 27, 447–452 (in Chinese with English abstract).
Yu, H.L., Yuan, B.Y., Huang, W.W., 2010. Re-examination of the Yanjiagang Paleolithic campsite, northeastern China. Acta Anthropol. Sin. 29, 445–453 (in Chinese with English abstract).
Zhang, H.W., 2020. Evolution and Systematics of the Elephatidae (Mammalia, Proboscidea) from the Late Miocene to Recent. Unpublished Doctoral Dissertation. University of Bristol, Bristol.
Zhang, H.C., 2009. A review of the study of environmental changes and extinction of the *Mammuthus-Colelodonta* Fauna during the middle-late Late Pleistocene in NE China. Adv. Earth Sci. 24, 49–60 (in Chinese with English abstract).
Zhang, H.C., Chang, F.Q., Li, H.Y., et al., 2019. OSL and AMS ^{14}C Age of the most complete mammoth fossil skeleton from northeastern China and its paleoclimate significance. Radiocarbon 61, 347–358.
Zhang, L.M., Griggo, C., Dong, W., et al., 2016. Preliminary taphonomic analyses on the mammalian remains from Wulanmulun Paleolithic site, Nei Mongol, China. Quat. Int. 400, 158–165.
Zhao, Y., Yu, Z., Herzschuh, U., et al., 2014. Vegetation and climate change during marine isotope stage 3 in China. Chin. Sci. Bull. 59, 4444–4455.
Zhou, W.J., Head, M.J., Deng, L., 2001. Climate changes in northern China since the late Pleistocene and its response to global change. Quat. Int. 83, 285–292.
Zimov, S.A., Zimov, N.S., Tikhonov, A.N., et al., 2012a. Mammoth steppe: a high-productivity phenomenon. Quat. Sci. Rev. 57, 26–45.
Zimov, S.A., Zimov, N.S., Chapin, F.S., 2012b. The Past and future of the mammoth steppe ecosystem. In: Louys, J. (Ed.), Paleontology in Ecology and Conservation. Springer Berlin Heidelberg, Berlin, Heidelberg, pp. 193–225.